

# *CP* Violation with $b$ hadrons at LHCb

*Laurence Carson, University of Edinburgh*

*on behalf of the LHCb collaboration*

*52<sup>nd</sup> Rencontres de Moriond, 22.03.17*

# CPV with $b$ Hadrons: Why?

- Sources of  $CPV$  beyond the Standard Model are needed to explain the large matter/antimatter asymmetry observed in the universe.
- Decays of  $b$  hadrons are an excellent place to search for new sources of  $CPV$ , as there is a rich variety of possible decays, some of which exhibit considerable  $CPV$  even in the SM.
- $CPV$  in hadrons can be classified into three distinct types:

<p>(A) <math>\left  \begin{array}{c} P \text{ --- } \bigcirc \text{ --- } f \end{array} \right ^2 \neq \left  \begin{array}{c} \bar{P} \text{ --- } \bigcirc \text{ --- } \bar{f} \end{array} \right ^2</math></p>	<p>(A) <math>CPV</math> in decay: difference in rate for a process and its charge conjugate, e.g. compare <math>B^+</math> and <math>B^-</math> decays.</p>
<p>(B) <math>\left  \begin{array}{c} P \text{ --- } \bullet \text{ --- } \bar{P} \text{ --- } \bigcirc \text{ --- } \bar{f} \end{array} \right ^2 \neq \left  \begin{array}{c} \bar{P} \text{ --- } \bullet \text{ --- } P \text{ --- } \bigcirc \text{ --- } f \end{array} \right ^2</math></p>	<p>(B) <math>CPV</math> in mixing: difference in rate between e.g. <math>B_s - \bar{B}_s</math> mixing vs <math>\bar{B}_s - B_s</math> mixing.</p>
<p>(C) <math>\left  \begin{array}{c} P \text{ --- } \bigcirc \text{ --- } f \\ + \\ P \text{ --- } \bullet \text{ --- } \bar{P} \text{ --- } \bigcirc \text{ --- } f \end{array} \right ^2 \neq \left  \begin{array}{c} \bar{P} \text{ --- } \bigcirc \text{ --- } f \\ + \\ \bar{P} \text{ --- } \bullet \text{ --- } P \text{ --- } \bigcirc \text{ --- } f \end{array} \right ^2</math></p>	<p>(C) <math>CPV</math> in interference between mixing and decay: typically gives rise to several <math>CPV</math> observables, requiring a time-dependent analysis of decay rates to disentangle them.</p>

# Menu of Results

**NEW!**

LHCb-PAPER-2017-008  
(in preparation)

LHCb-CONF-2016-014

LHCb-CONF-2016-015

LHCb-CONF-2016-018

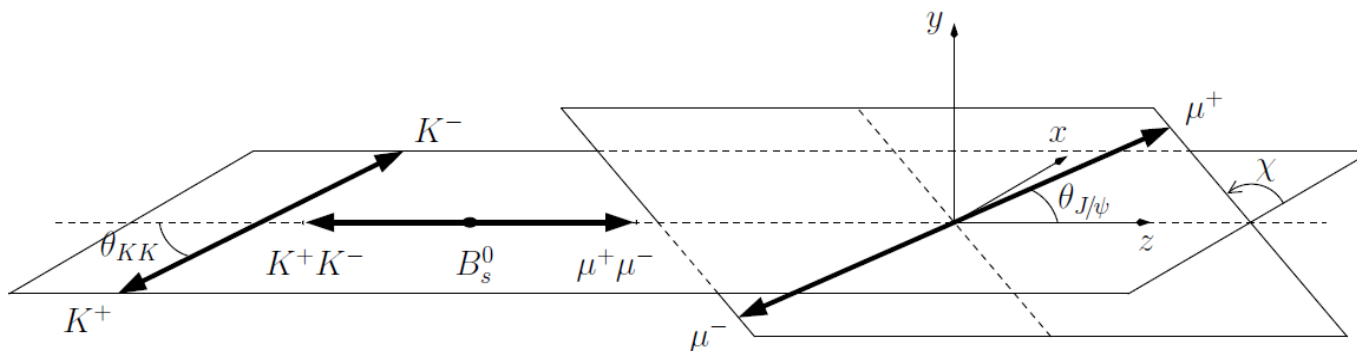
- First measurement of the  $CP$ -violating phase  $\phi_s$  using  $B_s^0 \rightarrow J/\psi K^+ K^-$  decays with  $m_{KK}$  above the  $\phi(1020)$  region
- First measurement of the CKM angle  $\gamma$  in the decay  $B^- \rightarrow D^0 K^{*-}$
- Updated measurement of  $\gamma$  using a time-dependent analysis of the decays  $B_s^0 \rightarrow D_s^\pm K^\mp$
- Updated time-dependent measurement of  $CP$ -violating observables in the decays  $B_d^0 \rightarrow \pi^+ \pi^-$  and  $B_s^0 \rightarrow K^+ K^-$

# The CP-Violating Phase $\phi_s$

- The SM prediction for  $\phi_s$ , the CP-violating phase in  $b \rightarrow c\bar{c}s$  transitions, is:

$$\phi_s^{\text{SM}} \equiv -2\arg\left(-\frac{V_{ts}V_{tb}^*}{V_{cs}V_{cb}^*}\right) = -37.6_{-0.7}^{+0.8} \text{ mrad} \quad \text{PRD 91 (2015) 073007}$$

- This prediction ignores corrections from penguin (loop) diagrams, which LHCb analyses have shown to be small. PLB 742 (2015) 38, JHEP 11 (2015) 082
- LHCb has measured  $\phi_s$  using  $B_s^0 \rightarrow J/\psi K^+ K^-$  decays with  $m_{KK}$  in the  $\phi(1020)$  region, and with  $B_s^0 \rightarrow J/\psi \pi^+ \pi^-$  decays, yielding a combined value of  $\phi_s = -10 \pm 39$  mrad. PRL 114 (2015) 041801, PLB 736 (2014) 186

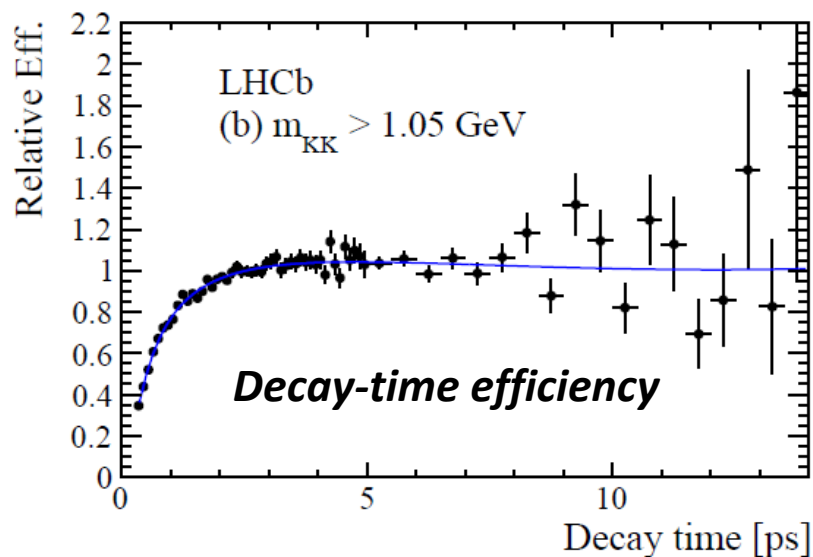
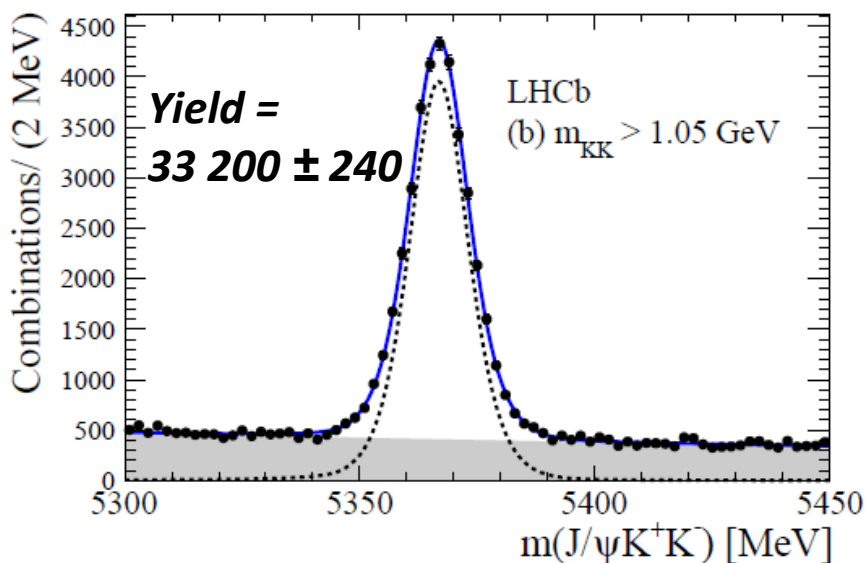


Definition of helicity angles for  $B_s^0 \rightarrow J/\psi K^+ K^-$

- LHCb also published an amplitude analysis of  $B_s^0 \rightarrow J/\psi K^+ K^-$  decays with  $m_{KK}$  above the  $\phi(1020)$  region, using 1/fb of data. However,  $\phi_s$  was not measured in this analysis. PRD 87 (2013) 072004

# New LHCb Measurement of $\phi_s$

- Now, a flavour-tagged, time-dependent amplitude analysis of  $B_s^0 \rightarrow J/\psi K^+ K^-$  with  $m_{KK}$  above the  $\phi(1020)$  region has been performed, using the full 3/fb of Run1 data.  
LHCb-PAPER-2017-008 (in preparation) **NEW!**
- Each vector or tensor resonance is allowed to contribute both  $CP$ -even and  $CP$ -odd decay amplitudes.
- Selection combines cut on a BDT classifier (combining kinematic/geometric variables and  $\mu$  PID) and cuts on hadron PID.
- The reconstruction and selection efficiency vs decay time is measured on data, using  $B_d^0 \rightarrow J/\psi K^{*0}(\rightarrow K^+ \pi^-)$  as a control channel.

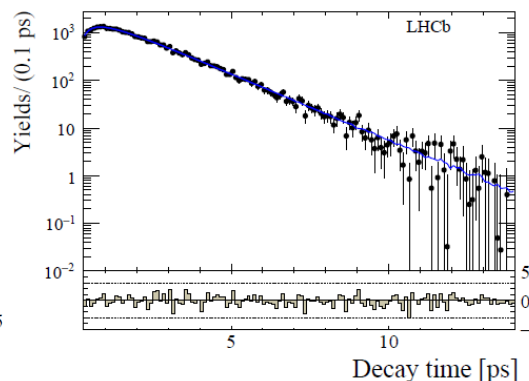
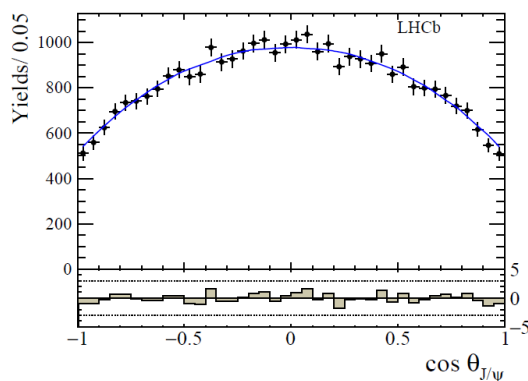




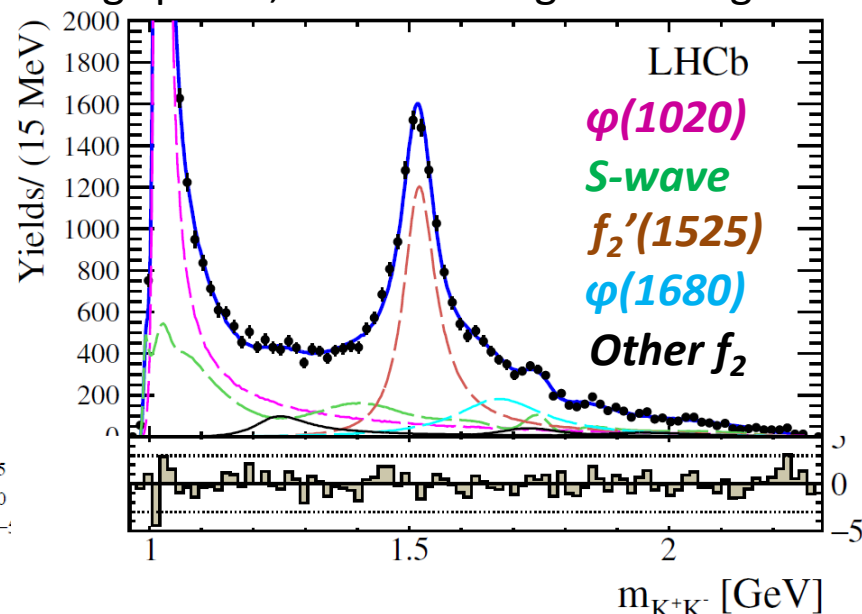
# New LHCb Measurement of $\phi_s$

- The fit to  $m(J/\psi K^+ K^-)$  is used to provide *sWeights* that are then used in a multi-dimensional fit to the decay time,  $m_{KK}$  and helicity angles.
- The flavour tagging uses both opposite-side (OS) and same-side Kaon (SSK) taggers.

Fit projections in  $\cos \theta_{J/\psi}$  and in decay time, for  $m_{KK} > 1.05$  GeV



Fit projection in  $m_{KK}$ . S-wave is modelled using splines, the rest using Breit-Wigners

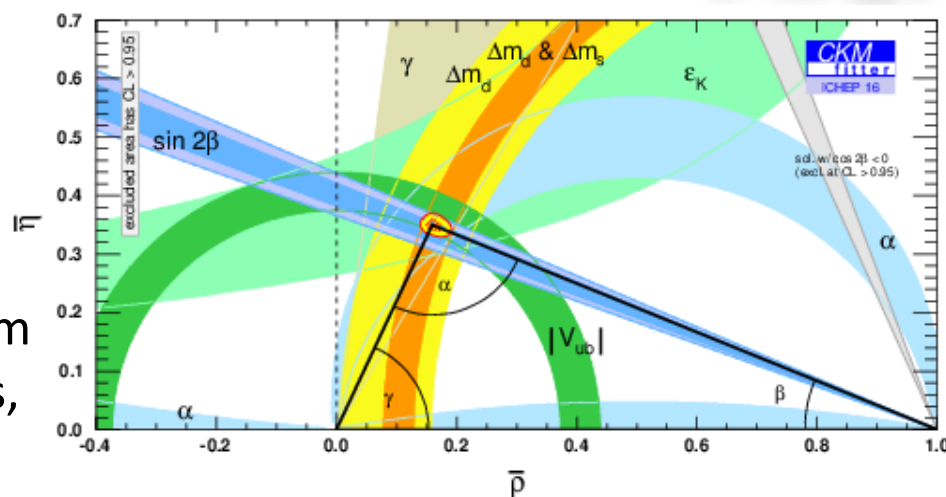


- For  $m_{KK} > 1.05$  GeV, we measure  $\phi_s = 0.12 \pm 0.11 \pm 0.03$  rad.
- Dominant systematics are from resonance modelling and background subtraction.
- Combining this with the previous LHCb measurements using  $B_s^0 \rightarrow J/\psi K^+ K^-$  and  $B_s^0 \rightarrow J/\psi \pi^+ \pi^-$  yields  $\phi_s = 0.001 \pm 0.037$  rad.

# The CKM Angle $\gamma$

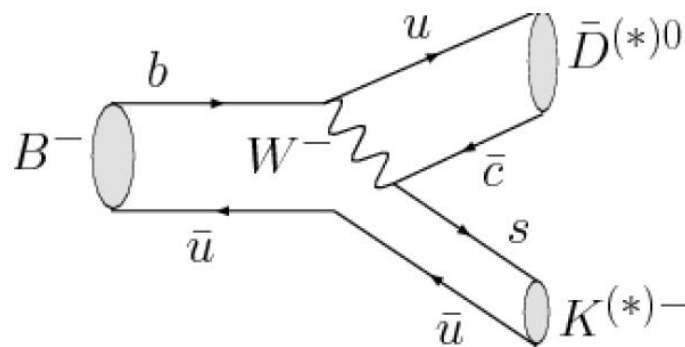
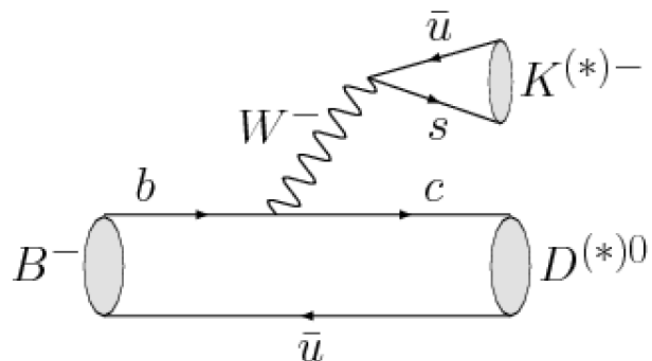
- This is the least well-constrained of the CKM angles. Combining all direct measurements yields  $\gamma = (72.1^{+5.4}_{-5.8})^\circ$ , while the latest LHCb-only combination (JHEP **12** (2016) 087) gives  $\gamma = (72.2^{+6.8}_{-7.3})^\circ$ .
- Indirect constraints from the other CKM parameters give  $\gamma = (65.3^{+1.0}_{-2.5})^\circ$ .
- Measurements of  $\gamma$  from  $B$  decays that are mediated only by tree-level transitions provide a “standard candle” for the Standard Model.
- This can be compared with  $\gamma$  values from  $B$  decays involving loop-level transitions, such as  $B_{d,s}^0 \rightarrow hh'$  decays ( $h = \{K, \pi\}$ ).
- Significant difference between these would indicate New Physics contribution to the loop process.
- Experimental methods to measure  $\gamma$  can be classified into time-independent and time-dependent.

$$\gamma = -\arg\left(\frac{V_{ud}V_{ub}^*}{V_{cd}V_{cb}^*}\right)$$



# CPV in $B^- \rightarrow D^0 K^{*-}$

- Time-independent measurements of  $\gamma$  exploit interference between  $b \rightarrow c$  and  $b \rightarrow u$  transitions in  $B^- \rightarrow \bar{D}^0 K^-$  decays. The exact analysis method depends on the  $D$  final state (use “ $D$ ” to stand for  $D^0$  or  $\bar{D}^0$ ).

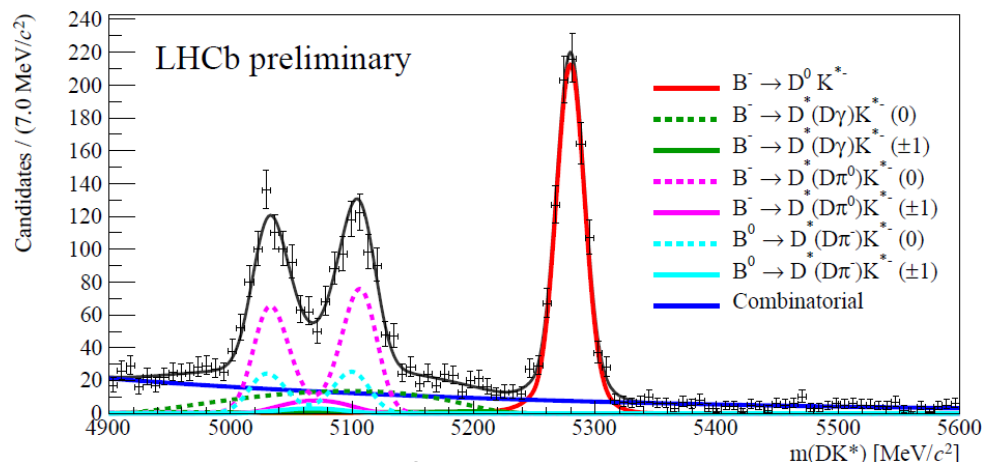


- LHCb is always seeking to improve the precision on  $\gamma$  by including new decay modes beyond the “classic”  $B^- \rightarrow DK^-$ .
- Recently, LHCb made the first measurement of the CPV observables in the decay  $B^- \rightarrow DK^{*-}$ . LHCb-CONF-2016-014
- The  $D^0$  final states used are  $K^- \pi^+$ ,  $K^+ K^-$ ,  $\pi^+ \pi^-$  and  $K^+ \pi^-$  (so-called ADS/GLW analysis) and the  $K^{*-}$  is reconstructed in the  $K_S^0 \pi^-$  final state.
- This analysis uses the full Run1 dataset, **plus** 1.0/fb of Run2 data (full 2015 dataset plus ~half of the 2016 dataset), giving a total of 4.0/fb.



# CPV in $B^- \rightarrow D^0 K^{*-}$

- Geometric, kinematic and isolation variables are combined to create a BDT classifier, used alongside hadron PID cuts.
- CP observables are extracted via a simultaneous fit to the different  $D$  decay modes.



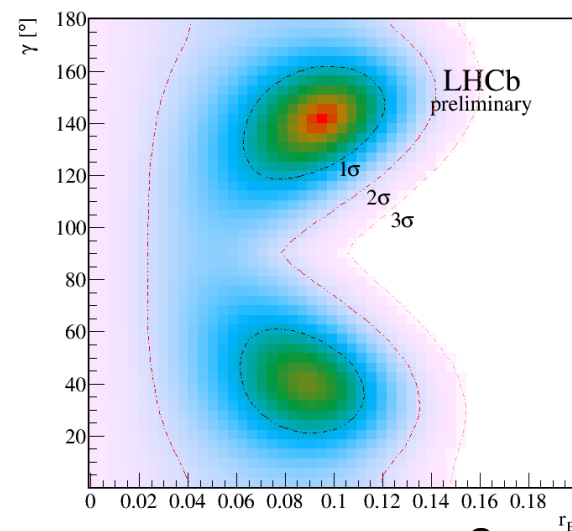
Run1+2 data,  $D^0 \rightarrow K^- \pi^+$  (favoured decay)

- Sensitivity to  $\gamma$  comes from combining  $D$  decay modes, such as (ADS case):

$$R^- = \frac{\Gamma(B^- \rightarrow D(K^+ \pi^-) K^{*-})}{\Gamma(B^- \rightarrow D(K^- \pi^+) K^{*-})} \quad R^+ = \frac{\Gamma(B^+ \rightarrow D(K^- \pi^+) K^{*+})}{\Gamma(B^+ \rightarrow D(K^+ \pi^-) K^{*+})}$$

$$R^\pm = \frac{r_B^2 + r_D^2 + 2\kappa r_B r_D \cos(\delta_B + \delta_D \pm \gamma)}{1 + r_B^2 r_D^2 + 2\kappa r_B r_D \cos(\delta_B - \delta_D \pm \gamma)}$$

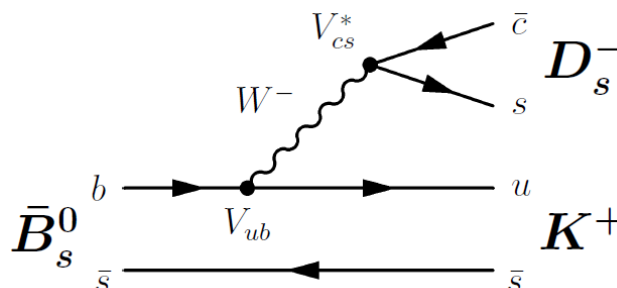
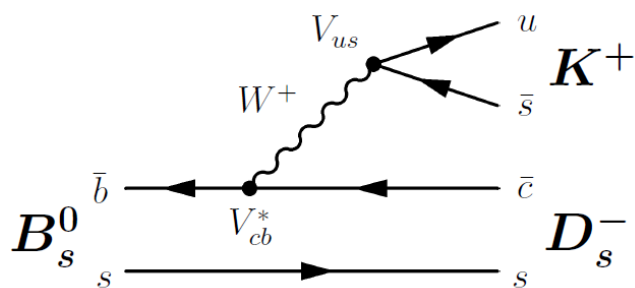
- Here, the ratio of suppressed to favoured  $B(D)$  decay amplitudes is  $r_B e^{i(\delta_{B^-} - \gamma)} (r_D e^{i\delta_D})$ .
- Plan to follow preliminary result with analysis including full 2016 dataset.



# $\gamma$ from $B_s^0 \rightarrow D_s^\pm K^\mp$

- The fact that  $B_s^0$  and  $\bar{B}_s^0$  can each decay to both  $D_s^- K^+$  and  $D_s^+ K^-$  means that a flavour-tagged, time-dependent analysis of these decays can give access to  $\gamma$ .
- LHCb recently updated this measurement of  $\gamma$ , using the full Run1 dataset.

LHCb-CONF-2016-015



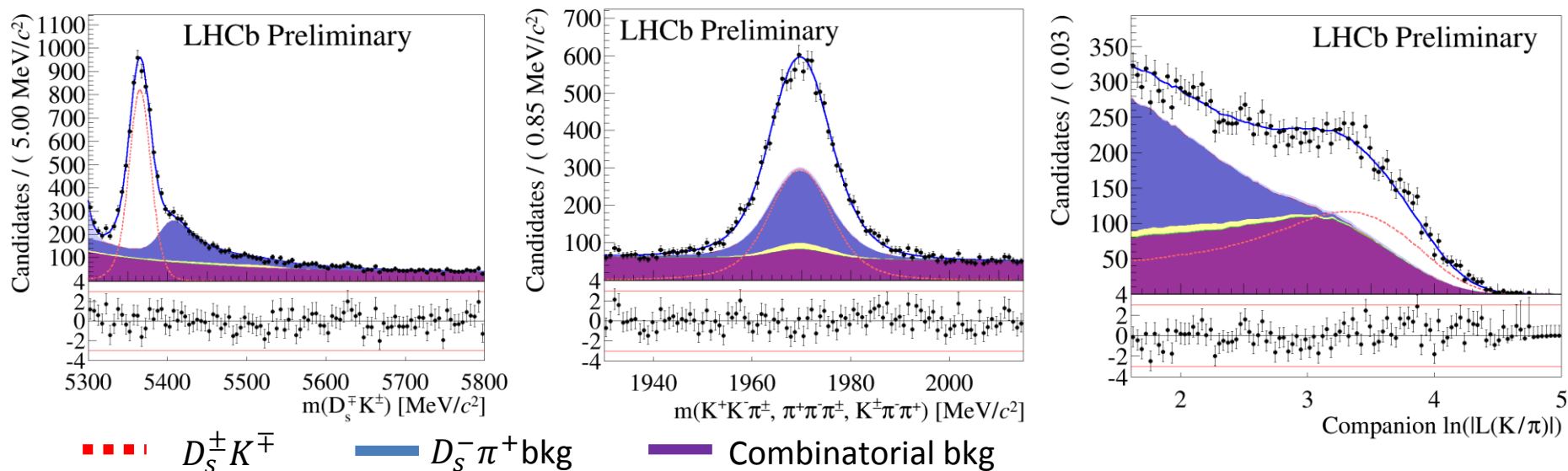
$$\frac{d\Gamma_{B_s^0 \rightarrow f}(t)}{dt} \propto e^{-\Gamma_s t} \left[ \cosh\left(\frac{\Delta\Gamma_s t}{2}\right) + A_f^{\Delta\Gamma} \sinh\left(\frac{\Delta\Gamma_s t}{2}\right) \oplus C_f \cos(\Delta m_s t) \ominus S_f \sin(\Delta m_s t) \right],$$

$$\frac{d\Gamma_{\bar{B}_s^0 \rightarrow f}(t)}{dt} \propto e^{-\Gamma_s t} \left[ \cosh\left(\frac{\Delta\Gamma_s t}{2}\right) + A_f^{\Delta\Gamma} \sinh\left(\frac{\Delta\Gamma_s t}{2}\right) \ominus C_f \cos(\Delta m_s t) \oplus S_f \sin(\Delta m_s t) \right]$$

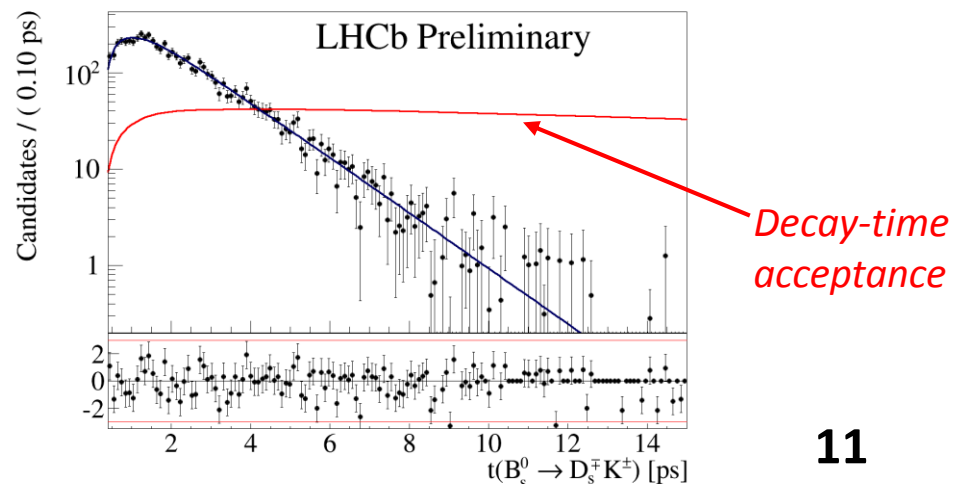
- The  $D_s^-$  is reconstructed in the  $K^- K^+ \pi^-$ ,  $\pi^- \pi^+ \pi^-$  and  $K^- \pi^+ \pi^-$  final states.
- The flavour-specific control channel  $B_s^0 \rightarrow D_s^- \pi^+$  is used to determine the decay-time-dependent efficiencies and the flavour-tagging performance, and to train the BDT classifier.

# $\gamma$ from $B_S^0 \rightarrow D_S^\pm K^\mp$

- A 3-dimensional fit is made to the  $D_S^- K^+$  mass, the  $D_S^-$  mass and the PID likelihood of the companion Kaon.



- This 3D fit provides *sWeights* used to subtract the backgrounds in the time-dependent fit for the *CPV* observables.
- The *CPV* fit constrains  $\Gamma_S$ ,  $\Delta\Gamma_S$  and  $\Delta m_S$  to their HFAG averages.
- Both OS and SSK taggers are used.

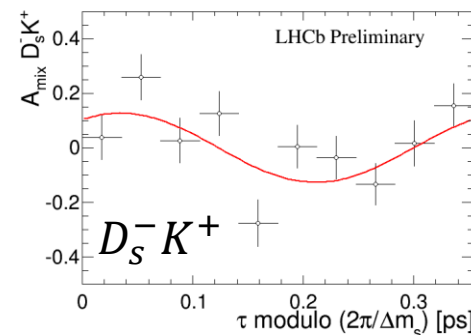
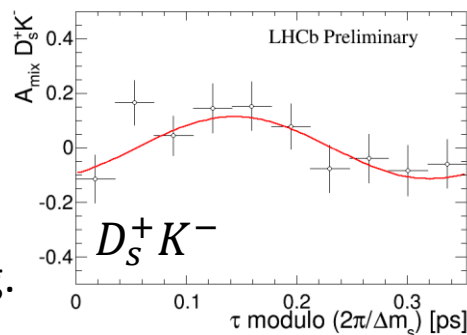


# $\gamma$ from $B_s^0 \rightarrow D_s^\pm K^\mp$

- The CPV observables fit gives:

Parameter	Value
$C_f$	$0.735 \pm 0.142 \pm 0.048$
$A_f^{\Delta\Gamma}$	$0.395 \pm 0.277 \pm 0.122$
$A_{\bar{f}}^{\Delta\Gamma}$	$0.314 \pm 0.274 \pm 0.107$
$S_f$	$-0.518 \pm 0.202 \pm 0.073$
$S_{\bar{f}}$	$-0.496 \pm 0.197 \pm 0.071$

Can visualise  $CP$  asymmetry by comparing (folded) oscillations of  $D_s^- K^+$  and  $D_s^+ K^-$ :

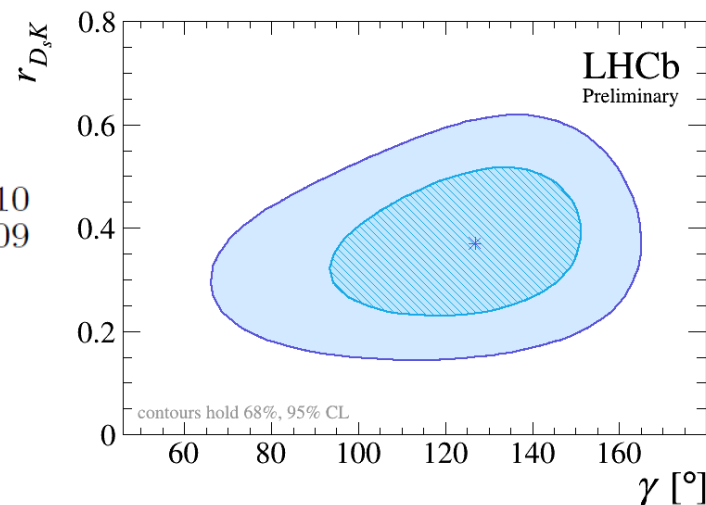


Dominant systematic varies by parameter, e.g.  $A_{det}$  or correlations between observables

- From these observables, use e.g.  $C_f = \frac{1 - r_{D_s K}^2}{1 + r_{D_s K}^2}$ ,  
 $S_f = \frac{2r_{D_s K} \sin(\delta - (\gamma - 2\beta_s))}{1 + r_{D_s K}^2}$  to obtain:

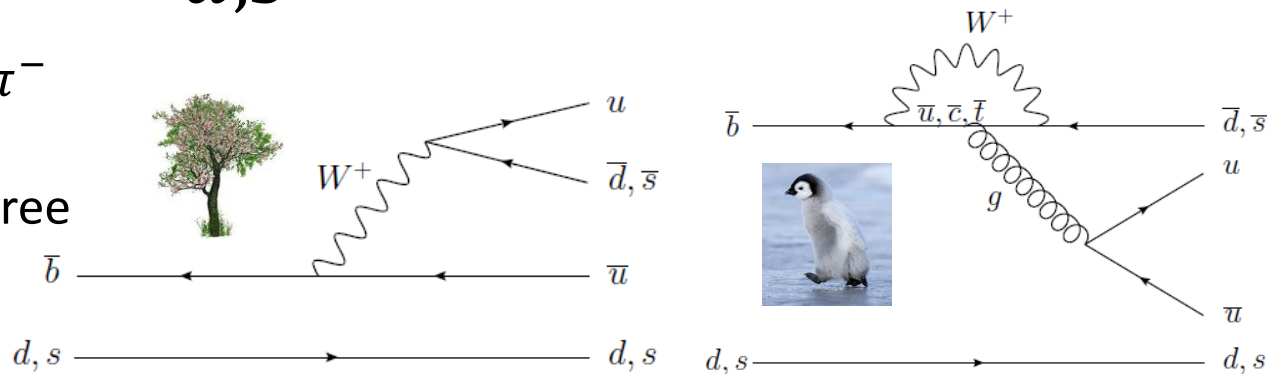
$$\gamma = (127_{-22}^{+17})^\circ, \quad \delta = (358_{-16}^{+15})^\circ, \quad r_{D_s K} = 0.37_{-0.09}^{+0.10}$$

- Here,  $r_{D_s K} = |A(\bar{B}_s^0 \rightarrow D_s^- K^+)/A(B_s^0 \rightarrow D_s^- K^+)|$  and  $\delta$  is the strong phase difference.
- Compatibility of  $\gamma$  with the previous combined LHCb measurement is  $2.2\sigma$ .



# $\gamma$ from $B_{d,s}^0 \rightarrow hh$ Decays

- Decays such as  $B_d^0 \rightarrow \pi^+ \pi^-$  and  $B_s^0 \rightarrow K^+ K^-$  receive contributions from both tree and penguin diagrams.



- A flavour-tagged, time-dependent analysis of these two modes allows CPV observables to be measured:

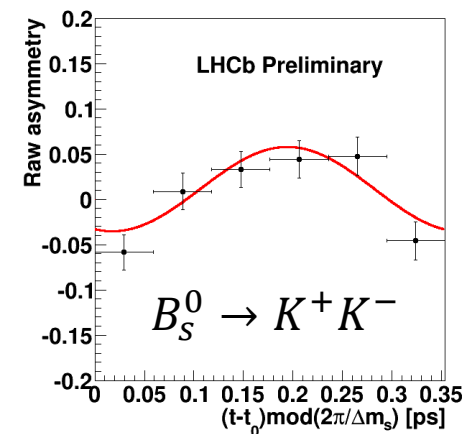
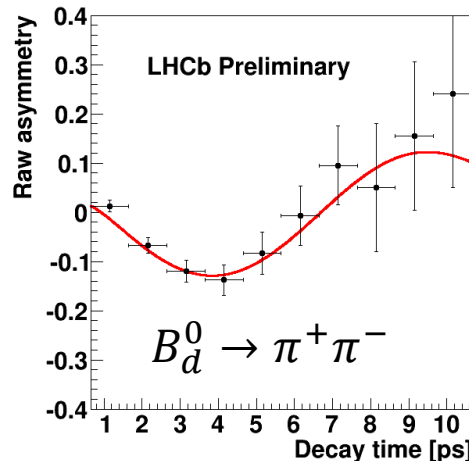
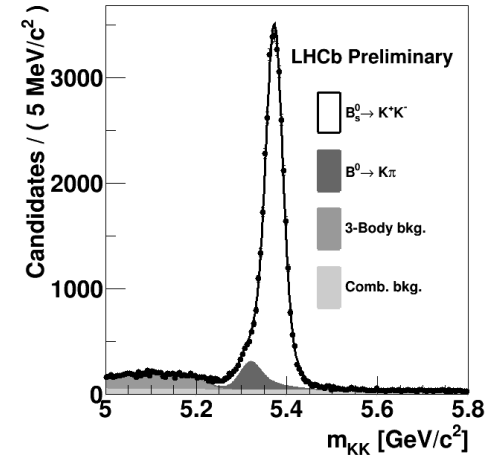
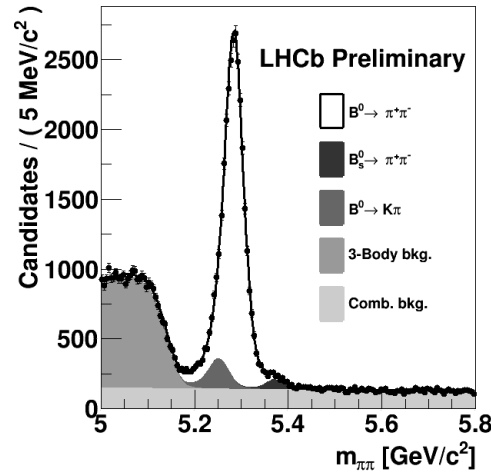
$$\mathcal{A}(t) = \frac{\Gamma_{\bar{B}_{(s)}^0 \rightarrow f}(t) - \Gamma_{B_{(s)}^0 \rightarrow f}(t)}{\Gamma_{\bar{B}_{(s)}^0 \rightarrow f}(t) + \Gamma_{B_{(s)}^0 \rightarrow f}(t)} = \frac{-C_f \cos(\Delta m_{d,s} t) + S_f \sin(\Delta m_{d,s} t)}{\cosh\left(\frac{\Delta \Gamma_{d,s}}{2} t\right) + A_f^{\Delta \Gamma} \sinh\left(\frac{\Delta \Gamma_{d,s}}{2} t\right)},$$

- These CPV observables can then be used to constrain  $\gamma$  and  $\phi_s$ , under certain assumptions (U-spin symmetry) relating the strong interaction dynamics of the two decays. **PLB 459 (1999) 306**
- LHCb recently updated its measurement of these observables, using the full Run1 dataset. **LHCb-CONF-2016-018**
- The control channel  $B_d^0 \rightarrow K^+ \pi^-$  is used to calibrate the flavour tagging.
- Only opposite-side taggers are used.



# $\gamma$ from $B_{d,s}^0 \rightarrow hh$ Decays

- Signal and backgrounds are parameterised in invariant mass, decay time and per-event mistag probability.
  - In the time-dependent fit  $\Gamma_{d,s}$ ,  $\Delta\Gamma_{d,s}$  and  $\Delta m_{d,s}$  are constrained to their HFAG averages.
- $$C_{\pi^+\pi^-} = -0.24 \pm 0.07 \pm 0.01,$$
- $$S_{\pi^+\pi^-} = -0.68 \pm 0.06 \pm 0.01,$$
- $$C_{K^+K^-} = 0.24 \pm 0.06 \pm 0.02,$$
- $$S_{K^+K^-} = 0.22 \pm 0.06 \pm 0.02,$$
- $$A_{K^+K^-}^{\Delta\Gamma} = -0.75 \pm 0.07 \pm 0.11,$$
- This gives strong evidence ( $4.7\sigma$ ) of CPV in  $B_s^0 \rightarrow K^+K^-$ .
  - Updated analysis is planned that will include same-side taggers and update constraints on  $\gamma$ .



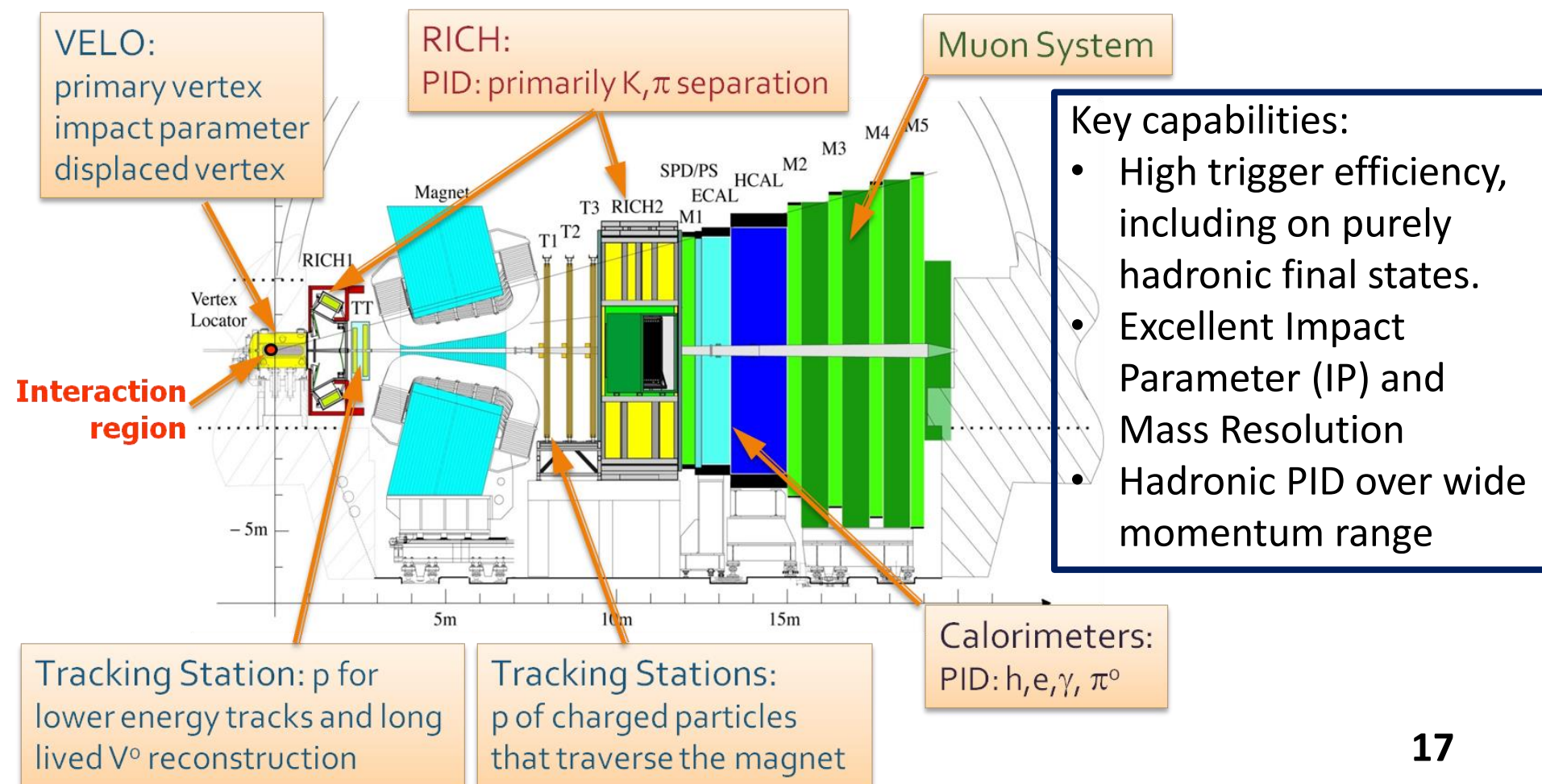
# Summary

- LHCb has made the first measurement of  $\phi_s$  using  $B_s^0 \rightarrow J/\psi K^+ K^-$  decays at high  $m_{KK}$ , giving a new LHCb combined value of  **$\phi_s = 0.001 \pm 0.037$  rad.**
- LHCb is producing new results improving the constraints on  $\gamma$ , both from tree-only decays and those involving loops.
- Another  $\approx 3/\text{fb}$  of data will have been collected by the end of LHC Run2 (2018), allowing for more precise *CPV* measurements in existing channels, and for new channels to be explored for the first time.
- LHCb aims to achieve a combined precision on  $\gamma$  of  $\approx 4^\circ$  by the end of Run2, and  $< 1^\circ$  by the end of Run4 (2029).
- Stay tuned for more results in the near future!
  - First *CPV* analyses using Run2 data are starting to appear
  - Many many more are in the pipeline...

# Backups

# The LHCb Experiment

- Forward arm spectrometer, optimised for study of  $B$  and  $D$  decays.
- Collected 1/fb of data at  $E_{\text{CM}} = 7$  TeV in 2011, 2/fb at 8 TeV in 2012, and 2/fb at 13 TeV in 2015 & 2016.

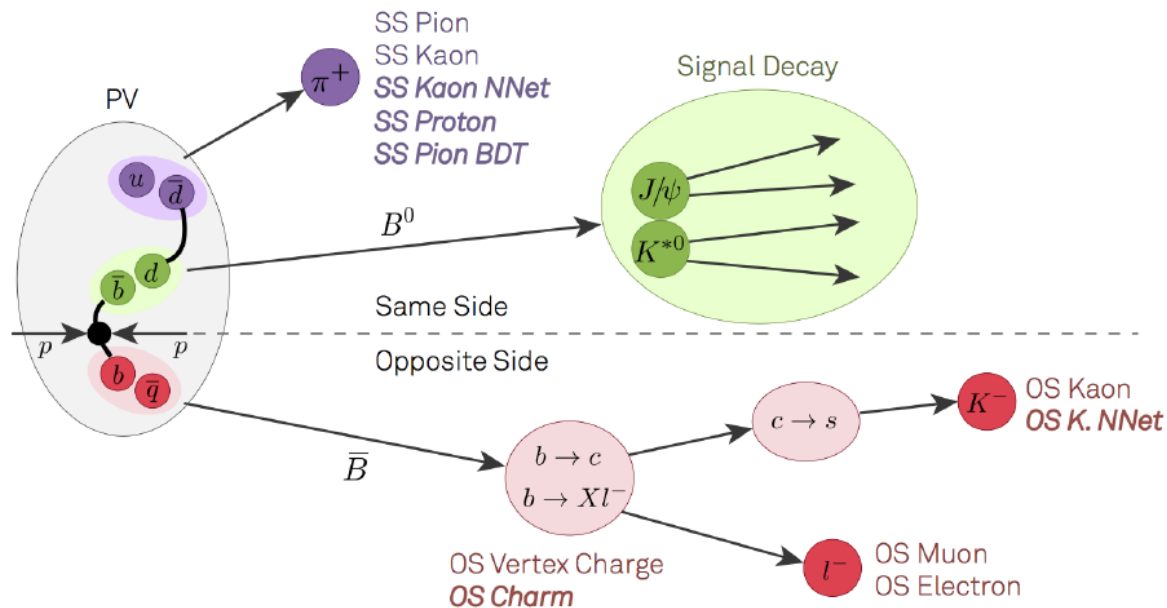


# Flavour Tagging

- Flavour tagging can be opposite side (OS) or same-side (SS).
- The tagging efficiency  $\epsilon_{tag}$  and the mistag rate  $\omega$  are defined as:

$$\epsilon_{tag} = \frac{N_{tag}}{N_{tag} + N_{untag}},$$

$$\omega = \frac{N_{wrong}}{N_{right} + N_{wrong}}$$



- The tagging power is then:  $\epsilon_{eff} = \epsilon_{tag}(1 - 2\omega)^2$
- The statistical uncertainty is proportional to:  $\sigma_{stat} \propto \frac{1}{\sqrt{N\epsilon_{eff}}}$
- At LHCb,  $\epsilon_{eff}$  is typically up to  $\approx 5\%$ .



# The CKM Matrix

- The CKM matrix relates the quark flavour eigenstates ( $d', s', b'$ ) to the mass eigenstates ( $d, s, b$ ) :

$$\begin{pmatrix} d' \\ s' \\ b' \end{pmatrix} = V_{CKM} \begin{pmatrix} d \\ s \\ b \end{pmatrix} \quad V_{CKM} = \begin{pmatrix} V_{ud} & V_{us} & V_{ub} \\ V_{cd} & V_{cs} & V_{cb} \\ V_{td} & V_{ts} & V_{tb} \end{pmatrix}$$

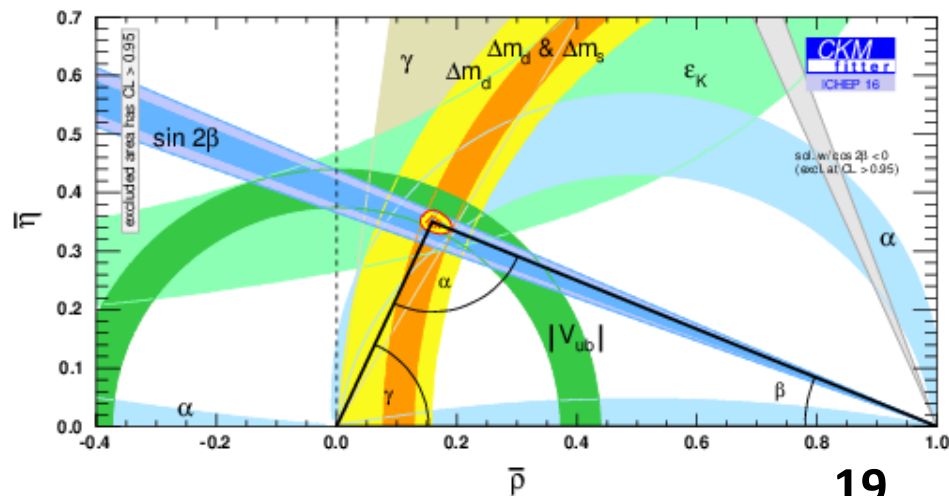
- The CKM triangle(s) come from the fact that the CKM matrix must be unitary.
- The CKM phase is the only source of *CPV* in (the quark sector of) the SM.

$$V_{ud}V_{ub}^* + V_{cd}V_{cb}^* + V_{td}V_{tb}^* = 0$$

## Wolfenstein parameterisation

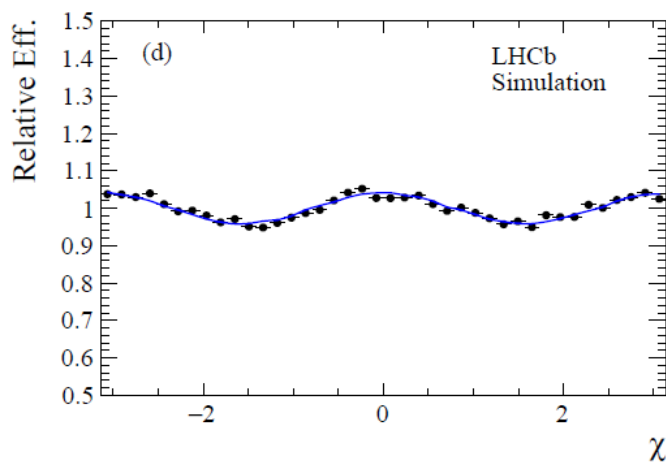
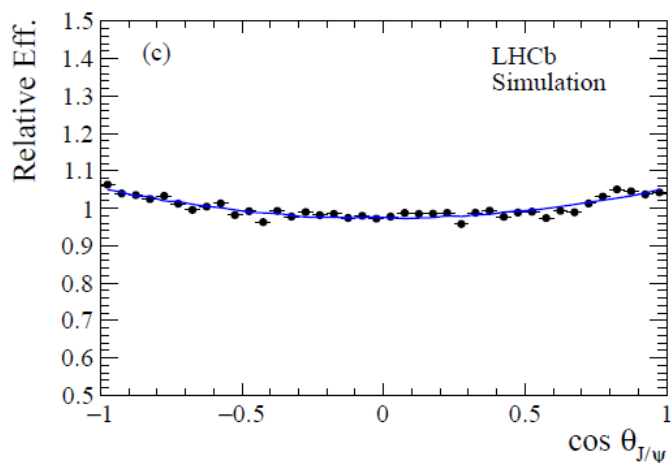
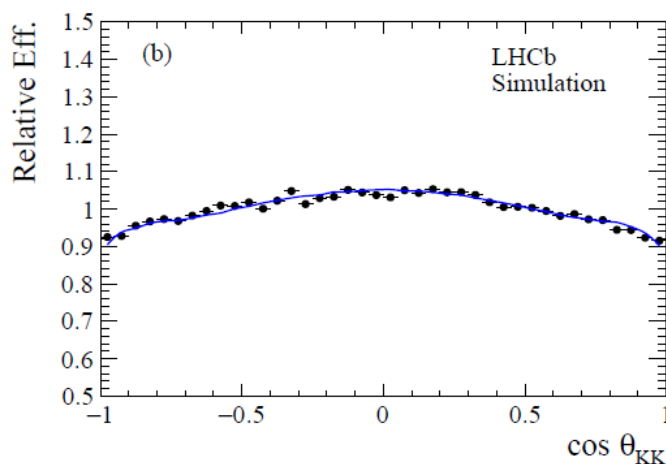
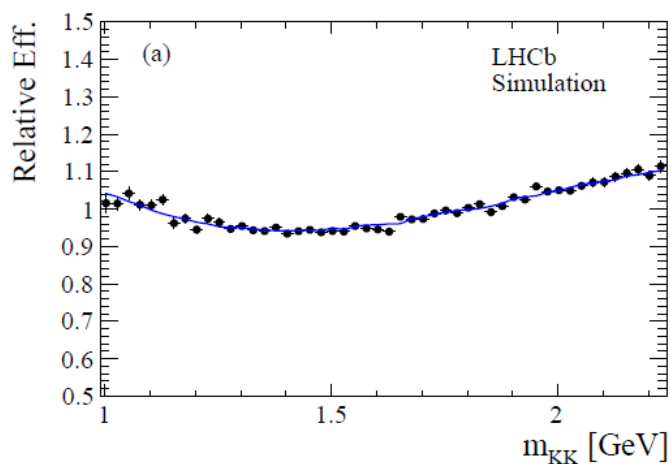
$$\begin{pmatrix} 1 - \frac{1}{2}\lambda^2 & \lambda & A\lambda^3(\rho - i\eta) \\ -\lambda & 1 - \frac{1}{2}\lambda^2 & A\lambda^2 \\ A\lambda^3(1 - \rho - i\eta) & -A\lambda^2 & 1 \end{pmatrix}$$

$$( \bar{\rho} \equiv \rho(1 - \lambda^2/2), \bar{\eta} \equiv \eta(1 - \lambda^2/2) )$$



# Efficiencies for $B_s^0 \rightarrow J/\psi K^+ K^-$

- The angular and  $m_{KK}$  efficiencies are determined using simulated phase-space decays of  $B_s^0 \rightarrow J/\psi K^+ K^-$ .



# Fit for $B_s^0 \rightarrow J/\psi K^+ K^-$

- The *sWeights* obtained from the  $J/\psi K^+ K^-$  mass fit are used to perform a 5D fit to the decay time,  $m_{KK}$  and the three helicity angles.

- The PDF is:

$$\mathcal{F}(t, m_{KK}, \Omega, \mathbf{q}|\eta, \delta_t) = [\mathcal{R}(\hat{t}, m_{KK}, \Omega, \mathbf{q}|\eta) \otimes T(t - \hat{t}|\delta_t)] \cdot \varepsilon_{\text{data}}^{B_s^0}(t) \cdot \varepsilon(m_{KK}, \Omega),$$

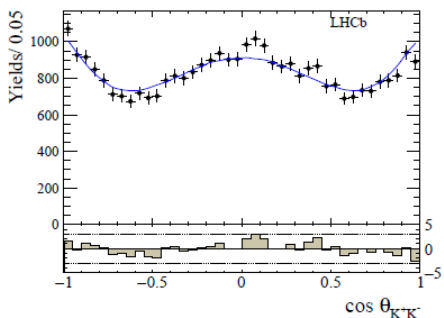
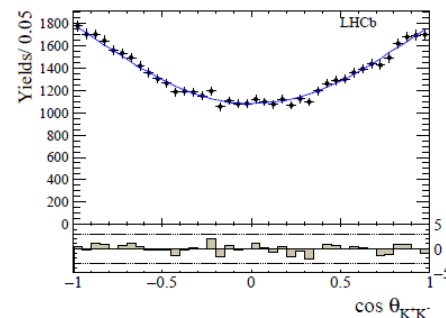
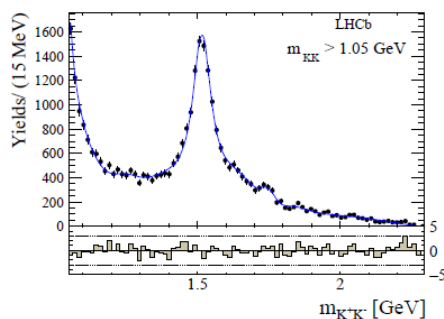
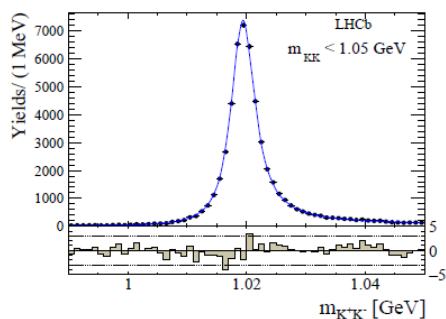
$$\text{with } \mathcal{R}(\hat{t}, m_{KK}, \Omega, \mathbf{q}|\eta) = \frac{1}{1 + |\mathbf{q}|} \left[ [1 + \mathbf{q} (1 - 2\omega(\eta))] \Gamma(\hat{t}, m_{KK}, \Omega) \right. \\ \left. + [1 - \mathbf{q} (1 - 2\bar{\omega}(\eta))] \frac{1 + A_P}{1 - A_P} \bar{\Gamma}(\hat{t}, m_{KK}, \Omega) \right]$$

- Here,  $\Omega$  represents the three helicity angles,  $\mathbf{q}$  is the flavour tag decision (+1, -1, or 0), and  $A_P = (1.1 \pm 2.7)\%$  is the  $B_s^0$  production asymmetry.

# Fit for $B_s^0 \rightarrow J/\psi K^+ K^-$

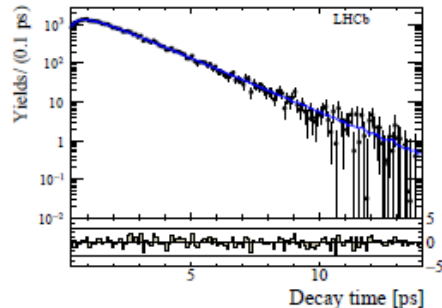
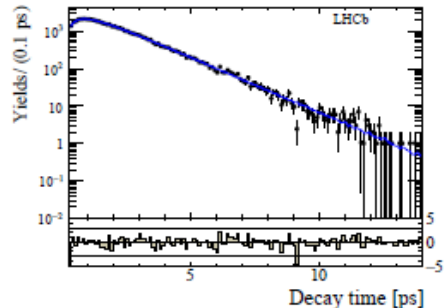
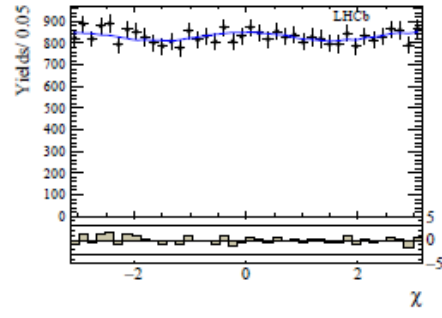
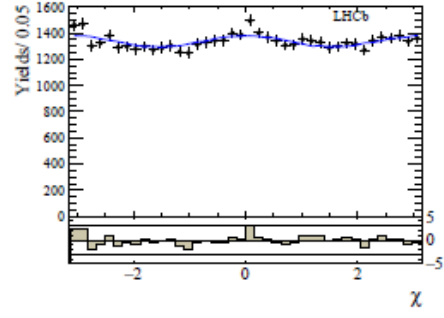
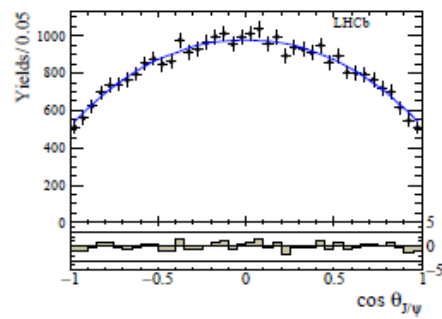
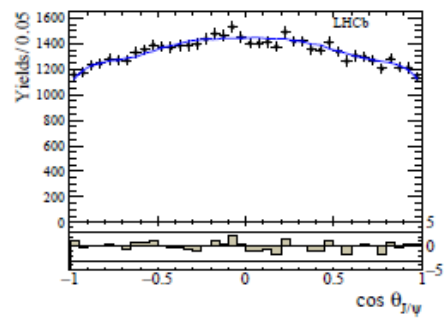
Left:  $\phi(1020)$  region

Right: higher  $m_{KK}$  region



Left:  $\phi(1020)$  region

Right: higher  $m_{KK}$  region



# Other Results from $B_s^0 \rightarrow J/\psi K^+ K^-$

- For  $m_{KK} > 1.05$  GeV, we measure  $\phi_s = 0.12 \pm 0.11 \pm 0.03$  rad ,  
(where  $\lambda \equiv \frac{q}{p} \frac{\bar{A}}{A}$ ):  $|\lambda| = 0.994 \pm 0.018 \pm 0.006$ ,  
 $\Gamma_s = 0.650 \pm 0.006 \pm 0.004$  ps<sup>-1</sup>,  
 $\Delta\Gamma_s = 0.066 \pm 0.018 \pm 0.010$  ps<sup>-1</sup>.

*Fitted phase differences between transversity states (stat. error only)*

States	Phase difference (°)
$f_2^0 - \phi^\perp$	$139.5 \pm 6.5$
$f_2'^0 - \phi^\perp$	$-167.9 \pm 6.6$
$f_2(1750)^0 - \phi^\perp$	$-251.5 \pm 13.0$
$f_2(1950)^0 - \phi^\perp$	$-84.1 \pm 42.1$
$\phi(1680)^0 - \phi^0$	$181.5 \pm 5.2$
$f_2^\perp - \phi^0$	$100.5 \pm 16.1$
$f_2'^\perp - \phi^0$	$-145.4 \pm 9.2$
$f_2(1750)^\perp - \phi^0$	$230.2 \pm 36.1$
$f_2(1950)^\perp - \phi^0$	$116.7 \pm 17.4$
$\phi^\perp - \phi^0$	$199.7 \pm 7.6$
$\phi(1680)^\perp - \phi^\perp$	$134.0 \pm 7.6$
$f_2^\parallel - \phi^\perp$	$-140.3 \pm 21.4$
$f_2'^\parallel - \phi^\perp$	$46.2 \pm 7.9$
$f_2(1750)^\parallel - \phi^\perp$	$-27.5 \pm 15.9$
$f_2(1950)^\parallel - \phi^\perp$	$3.8 \pm 19.5$
$\phi^\parallel - \phi^0$	$195.4 \pm 3.8$
$\phi(1680)^\parallel - \phi^0$	$-105.8 \pm 8.9$

*Results of fit to resonance structure. The dominant systematic is due to the modelling of the resonances themselves.*

Component	Fit fraction (%)	Transversity fraction (%)		
		0	$\parallel$	$\perp$
$\phi(1020)$	$70.5 \pm 0.6 \pm 1.2$	$50.9 \pm 0.4$	$23.1 \pm 0.5$	$26.0 \pm 0.6$
$f_2(1270)$	$1.6 \pm 0.3 \pm 0.2$	$76.9 \pm 5.5$	$6.0 \pm 4.2$	$17.1 \pm 5.0$
$f_2'(1525)$	$10.7 \pm 0.7 \pm 0.9$	$46.8 \pm 1.9$	$33.8 \pm 2.3$	$19.4 \pm 2.3$
$\phi(1680)$	$3.95 \pm 0.3 \pm 0.3$	$44.0 \pm 3.9$	$32.7 \pm 3.6$	$23.3 \pm 3.6$
$f_2(1750)$	$0.59^{+0.23}_{-0.16} \pm 0.21$	$58.2 \pm 13.9$	$31.7 \pm 12.4$	$10.1^{+16.8}_{-6.1}$
$f_2(1950)$	$0.44^{+0.15}_{-0.10} \pm 0.14$	$2.2^{+6.7}_{-1.5}$	$38.3 \pm 13.8$	$59.5 \pm 14.2$
<i>S</i> -wave	$10.69 \pm 0.12 \pm 0.57$	100	0	0



# Systematics for $B_s^0 \rightarrow J/\psi K^+ K^-$

Table 5: Absolute systematic uncertainties for the physics parameters, compared to the corresponding statistical uncertainty. Here  $M_0$  and  $\Gamma_0$  refer to the uncertainties on the  $f_2'(1525)$  resonance masse and width.

Source $\times 10^{-3}$	$\Delta\Gamma_s^H$ [ps $^{-1}$ ]	$\Gamma_s^H$ [ps $^{-1}$ ]	$ \lambda ^H$	$M_0$ [GeV]	$\Gamma_0$ [GeV]	$\phi_s^H$ [rad]
Res. modelling	6.9	1.9	5.5	1.1	3.6	23.6
Efficiency ( $m_{KK}, \Omega$ )	3.0	0.9	0.5	0.1	0.7	3.4
Efficiency $t$	2.2	2.8	0.0	0.0	0.0	0.0
$\tau_{\bar{B}^0}$	1.4	2.0	0.0	0.0	0.0	0.0
$t$ resolution	0.3	0.2	0.2	0.0	0.0	1.1
Bias	5.0	1.1	-	-	-	-
$A_{CP}^{\text{Prod}}$	0.1	0.3	1.4	0.0	0.0	4.0
Tagging	1.2	0.3	0.8	0.0	0.0	11.2
Backg.	0.5	0.8	0.4	0.1	0.1	1.5
Sweights	1.1	0.1	0.5	0.1	0.4	21.4
$B_c^+$	-	0.5	-	-	-	-
Total syst.	9.6	4.3	5.7	1.1	3.7	34.2
Stat.	17.7	5.5	18.0	1.3	3.0	106.6

Table 7: Total statistical and systematic correlation matrix from the high-mass region fit.

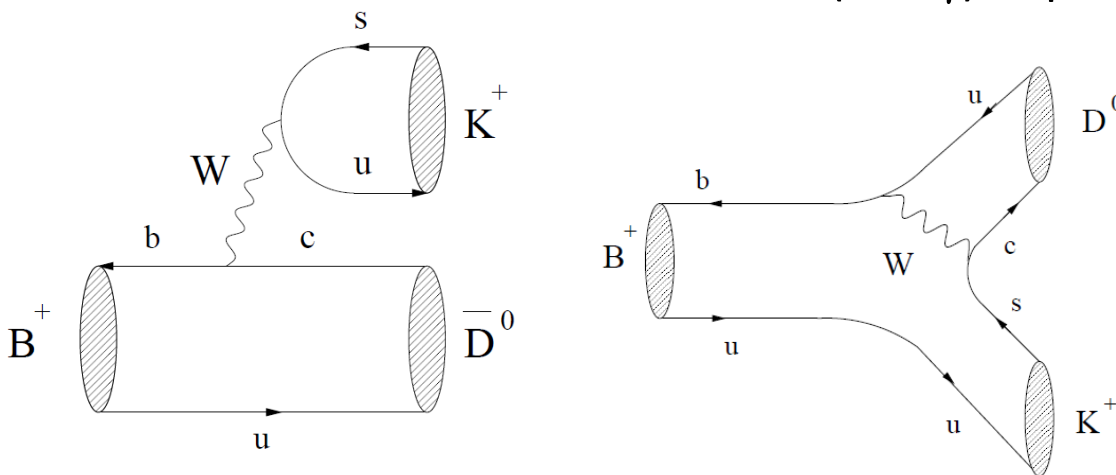
	$\Gamma_s$	$\Delta\Gamma_s$	$\phi_s$	$ \lambda $
$\Gamma_s$	+1.00	+0.54	+0.02	-0.03
$\Delta\Gamma_s$		+1.00	+0.04	-0.06
$\phi_s$			+1.00	-0.14
$ \lambda $				+1.00

Table 6: Absolute systematic uncertainty for fit fractions.

Source	$\phi(1020)$	$S$ -wave	$f_2'(1525)$	$\phi(1680)$	$f_2(1270)$	$f_2(1750)$	$f_2(1950)$
Res. modelling	0.99	0.57	0.73	0.27	0.21	0.21	0.13
Efficiency	0.58	0.06	0.48	0.12	0.04	0.03	0.01
Background	0.06	0.01	0.06	0.02	0.02	0.01	0.00
Sweights	0.11	0.02	0.16	0.05	0.02	0.05	0.04
Total syst.	1.15	0.57	0.89	0.30	0.21	0.21	0.14
Stat.	0.62	0.12	0.67	0.32	0.27	$^{+0.23}_{-0.16}$	$^{+0.15}_{-0.10}$

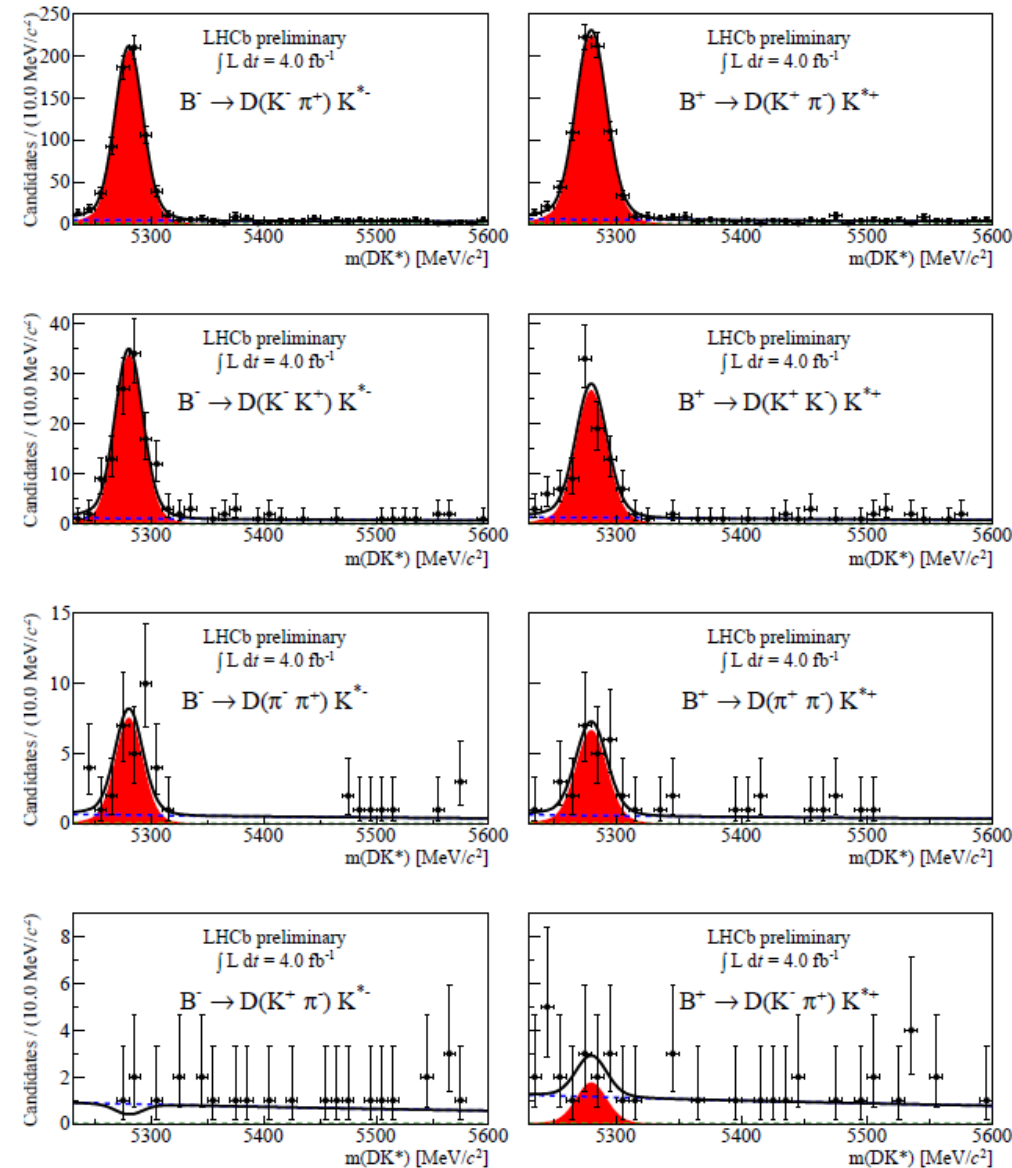
# Time-Integrated $\gamma$ Methods

- Aside from  $\gamma$ , have hadronic unknowns  $r_{B(D)}$ ,  $\delta_{B(D)}$ , where ratio of suppressed to favoured  $B(D)$  decay amplitudes is  $r_B e^{i(\delta_{B^-} - \gamma)} (r_D e^{i\delta_D})$
- Method to extract these hadronic unknowns (and  $\gamma$ ) depends on the  $D$  final state.



- Three main methods:
- GLW**:  $D \rightarrow CP$ -eigenstate, e.g.  $\pi\pi$ ,  $KK$  (Phys. Lett. **B 253** (1991) 483, Phys. Lett. **B 265** (1991) 172)
- ADS**:  $D \rightarrow$  quasi-flavour-specific state, e.g.  $K\pi$ ,  $K\pi\pi\pi$  (Phys. Rev. Lett. **78** (1997) 257, Phys. Rev. **D 63** (2001) 036005)
- GGSZ**:  $D \rightarrow$  self-conjugate 3-body final state, e.g.  $K_S\pi\pi$ ,  $K_S KK$  (Phys. Rev. **D 68** (2003) 054018, Phys. Rev. **D 70** (2004) 072003)

# Fits for $B^- \rightarrow D^0 K^{*-}$



$$A_{KK} = \frac{\Gamma(B^- \rightarrow D(KK)K^{*-}) - \Gamma(B^+ \rightarrow D(KK)K^{*+})}{\Gamma(B^- \rightarrow D(KK)K^{*-}) + \Gamma(B^+ \rightarrow D(KK)K^{*+})} = A_{CP+}$$

$$R_{KK} = \frac{\Gamma(B^- \rightarrow D(KK)K^{*-}) + \Gamma(B^+ \rightarrow D(KK)K^{*+})}{\Gamma(B^- \rightarrow D(K^- \pi^+)K^{*-}) + \Gamma(B^+ \rightarrow D(K^+ \pi^-)K^{*+})} \times \frac{B(D^0 \rightarrow K^- \pi^+)}{B(D^0 \rightarrow K^- K^+)} = R_{CP+}$$

$$A_{CP+} = \frac{2\kappa r_B \sin \delta_B \sin \gamma}{1 + r_B^2 + 2\kappa r_B \cos \delta_B \cos \gamma}$$

$$R_{CP+} = 1 + r_B^2 + 2\kappa r_B \cos \delta_B \cos \gamma$$

$$A_{K\pi} = -0.027 \pm 0.028 \, (\text{stat}) \pm 0.007 \, (\text{syst})$$

$$A_{KK} = 0.12 \pm 0.08 \, (\text{stat}) \pm 0.01 \, (\text{syst})$$

$$A_{\pi\pi} = 0.08 \pm 0.16 \, (\text{stat}) \pm 0.02 \, (\text{syst})$$

$$R_{KK} = 1.31 \pm 0.11 \, (\text{stat}) \pm 0.05 \, (\text{syst})$$

$$R_{\pi\pi} = 0.98 \pm 0.17 \, (\text{stat}) \pm 0.04 \, (\text{syst})$$

$$R^+ = 0.009 \pm 0.007 \, (\text{stat}) \pm 0.002 \, (\text{syst})$$

$$R^- = -0.003 \pm 0.004 \, (\text{stat}) \pm 0.002 \, (\text{syst}).$$

# Correlations & Systematics for $B^- \rightarrow D^0 K^{*-}$

Table 2: Summary of systematic uncertainties. Uncertainties are shown to be zero if they are more than two orders of magnitude smaller than the statistical error.

	$A_{K\pi}$	$A_{KK}$	$A_{\pi\pi}$	$R_{KK}$	$R_{\pi\pi}$	$R^+$	$R^-$
Statistical	0.028	0.08	0.16	0.11	0.17	0.007	0.004
BRs	0.0	0.0	0.0	$1.5 \times 10^{-2}$	$1.0 \times 10^{-2}$	0.0	0.0
MC efficiencies	0.0	$7.9 \times 10^{-4}$	$4.4 \times 10^{-3}$	$4.4 \times 10^{-2}$	$3.1 \times 10^{-2}$	$1.1 \times 10^{-4}$	$1.3 \times 10^{-4}$
PID efficiencies	0.0	0.0	0.0	$2.6 \times 10^{-3}$	0.0	0.0	0.0
Veto efficiencies	0.0	0.0	0.0	0.0	0.0	$1.1 \times 10^{-4}$	$1.2 \times 10^{-4}$
$A_{prod}$	$6.0 \times 10^{-3}$	$5.9 \times 10^{-3}$	$7.0 \times 10^{-3}$	0.0	0.0	0.0	0.0
$A_{det}$	$3.4 \times 10^{-3}$	$3.0 \times 10^{-3}$	$3.0 \times 10^{-3}$	0.0	0.0	0.0	0.0
Signal shape	$2.4 \times 10^{-3}$	$7.0 \times 10^{-3}$	$9.9 \times 10^{-3}$	$4.9 \times 10^{-3}$	$1.7 \times 10^{-2}$	$1.7 \times 10^{-3}$	$1.3 \times 10^{-3}$
Combinatorial shape	0.0	$6.4 \times 10^{-3}$	$3.8 \times 10^{-3}$	$4.5 \times 10^{-3}$	0.0	$3.0 \times 10^{-4}$	$1.4 \times 10^{-4}$
Partially reconstructed shape	0.0	$5.5 \times 10^{-3}$	$3.2 \times 10^{-3}$	0.0	$5.5 \times 10^{-3}$	$7.0 \times 10^{-4}$	$7.5 \times 10^{-4}$
Charmless	$3.4 \times 10^{-4}$	$4.0 \times 10^{-3}$	$4.7 \times 10^{-3}$	$1.4 \times 10^{-3}$	$5.7 \times 10^{-3}$	$6.2 \times 10^{-4}$	$7.2 \times 10^{-4}$
Total	0.0075	0.013	0.015	0.047	0.037	0.0020	0.0017

Table 3: Statistical correlation matrix for the seven physics observables from the simultaneous fit to data. For clarity, only half of the symmetric matrix is shown.

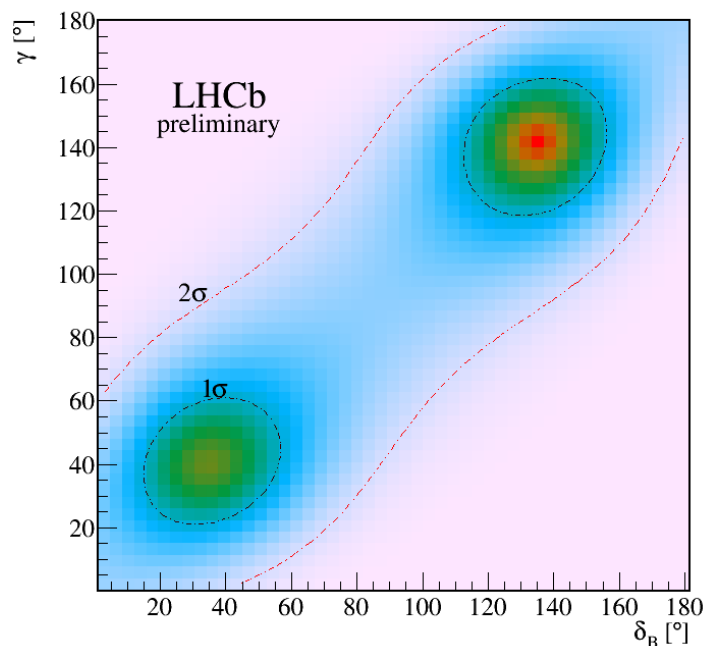
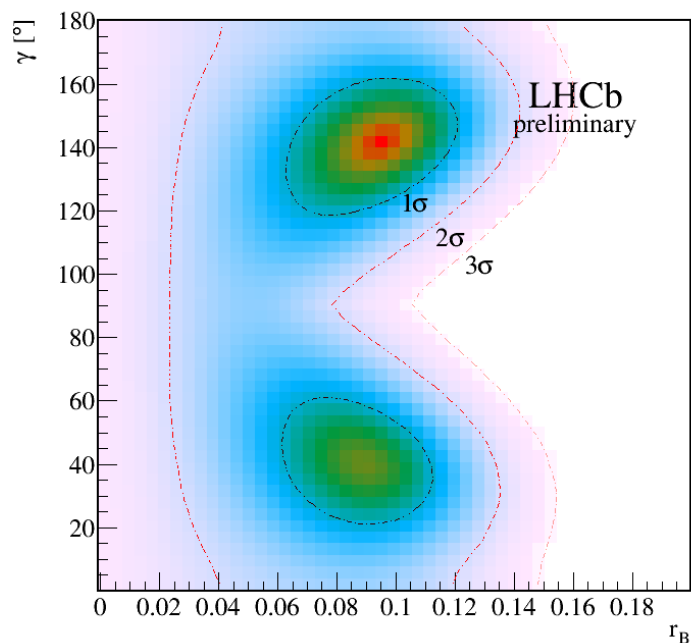
	$A_{K\pi}$	$A_{KK}$	$A_{\pi\pi}$	$R_{KK}$	$R_{\pi\pi}$	$R^+$	$R^-$
$A_{K\pi}$	1	0.00	0.00	0.00	0.00	0.04	0.02
$A_{KK}$		1	0.00	-0.02	0.00	-0.01	-0.01
$A_{\pi\pi}$			1	0.00	0.01	0.00	0.00
$R_{KK}$				1	0.06	0.03	0.01
$R_{\pi\pi}$					1	0.02	0.01
$R^+$						1	0.04
$R^-$							1

Table 4: Systematic correlation matrix for the seven physics observables from the simultaneous fit to data. For clarity, only half of the symmetric matrix is shown.

	$A_{K\pi}$	$A_{KK}$	$A_{\pi\pi}$	$R_{KK}$	$R_{\pi\pi}$	$R^+$	$R^-$
$A_{K\pi}$	1	0.46	0.52	0.00	0.00	0.01	-0.02
$A_{KK}$		1	0.41	-0.03	0.00	0.05	0.02
$A_{\pi\pi}$			1	-0.05	0.02	0.08	0.05
$R_{KK}$				1	-0.01	-0.01	0.00
$R_{\pi\pi}$					1	0.02	0.02
$R^+$						1	0.03
$R^-$							1

# Interpretation for $B^- \rightarrow D^0 K^{*-}$

- The parameters  $r_D$  and  $\delta_D$  are constrained to their HFAG averages.
- The coherence factor  $\kappa$  is estimated using a fit to the  $K_S^0 \pi^-$  mass distribution of selected events, yielding  $\kappa = 0.95 \pm 0.06$ .





# Relations for $B_s^0 \rightarrow D_s^\pm K^\mp$

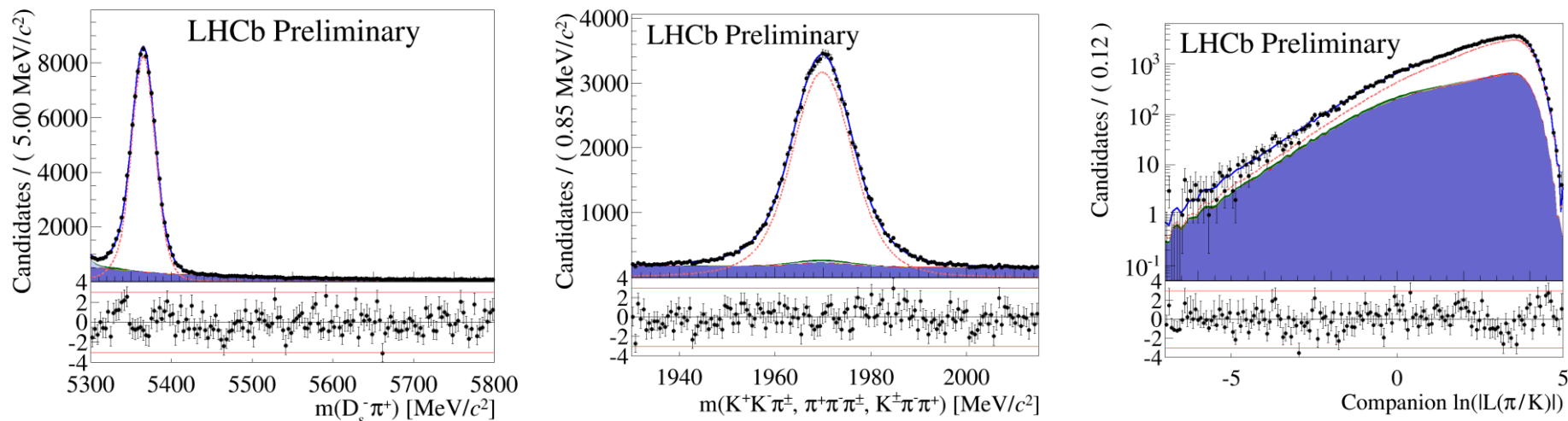
- These are the time-dependent decay rates.
 
$$\frac{d\Gamma_{B_s^0 \rightarrow f}(t)}{dt} \propto e^{-\Gamma_s t} \left[ \cosh\left(\frac{\Delta\Gamma_s t}{2}\right) + A_f^{\Delta\Gamma} \sinh\left(\frac{\Delta\Gamma_s t}{2}\right) + C_f \cos(\Delta m_s t) - S_f \sin(\Delta m_s t) \right],$$
- For decays to  $\bar{f}$ ,  $S_f$  is replaced by  $S_{\bar{f}}$ , and  $A_f$  by  $A_{\bar{f}}$ .
 
$$\frac{d\Gamma_{\bar{B}_s^0 \rightarrow \bar{f}}(t)}{dt} \propto e^{-\Gamma_s t} \left[ \cosh\left(\frac{\Delta\Gamma_s t}{2}\right) + A_{\bar{f}}^{\Delta\Gamma} \sinh\left(\frac{\Delta\Gamma_s t}{2}\right) - C_f \cos(\Delta m_s t) + S_f \sin(\Delta m_s t) \right],$$
- These observables are related to the physics parameters by:
 
$$C_f = \frac{1 - r_{D_s K}^2}{1 + r_{D_s K}^2},$$

$$A_f^{\Delta\Gamma} = \frac{-2r_{D_s K} \cos(\delta - (\gamma - 2\beta_s))}{1 + r_{D_s K}^2}, \quad A_{\bar{f}}^{\Delta\Gamma} = \frac{-2r_{D_s K} \cos(\delta + (\gamma - 2\beta_s))}{1 + r_{D_s K}^2},$$

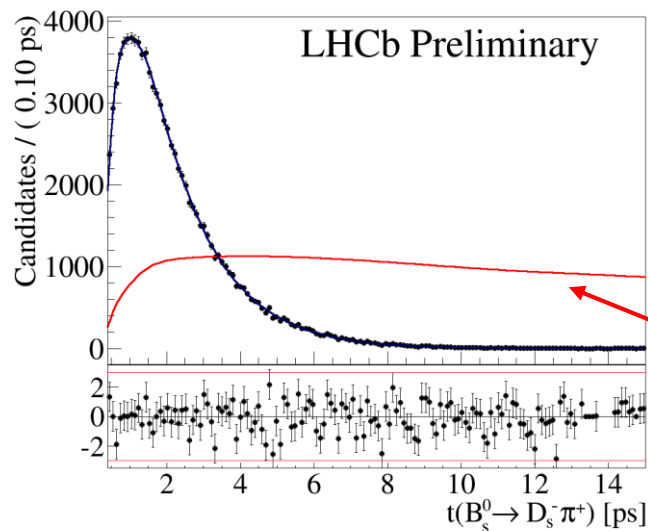
$$S_f = \frac{2r_{D_s K} \sin(\delta - (\gamma - 2\beta_s))}{1 + r_{D_s K}^2}, \quad S_{\bar{f}} = \frac{-2r_{D_s K} \sin(\delta + (\gamma - 2\beta_s))}{1 + r_{D_s K}^2}.$$
- Here,  $r_{D_s K} = |A(\bar{B}_s^0 \rightarrow D_s^- K^+)/A(B_s^0 \rightarrow D_s^- K^+)|$  and  $\delta$  is the strong phase difference.

# Fits to $B_S^0 \rightarrow D_S^- \pi^+$

- 3D fit to  $D_S^- \pi^+$  mass,  $D_S^-$  mass and the PID likelihood of the companion Pion:



- Decay-time fit, to give decay-time acceptance for  $B_S^0 \rightarrow D_S^\pm K^\mp$ :



Decay-time acceptance

# $B_s^0 \rightarrow D_s^\pm K^\mp$ Tagging Calibration

- Each event has a predicted mistag probability,  $\eta$ .
- A linear calibration function is used:  $\omega(\eta) = p_0 + p_1 \cdot (\eta - \langle \eta \rangle)$
- Calibrate using flavour-specific  $B_s^0 \rightarrow D_s^- \pi^+$ :

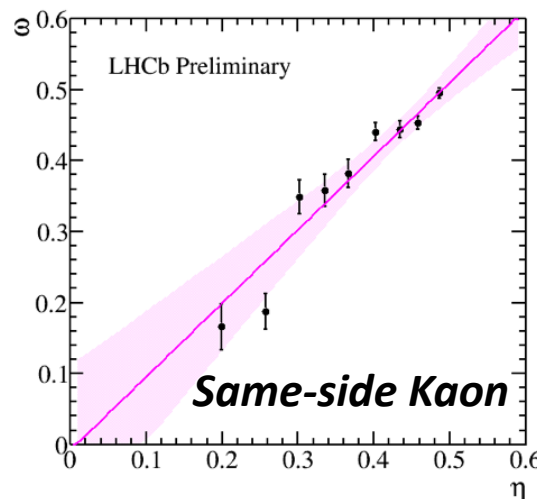
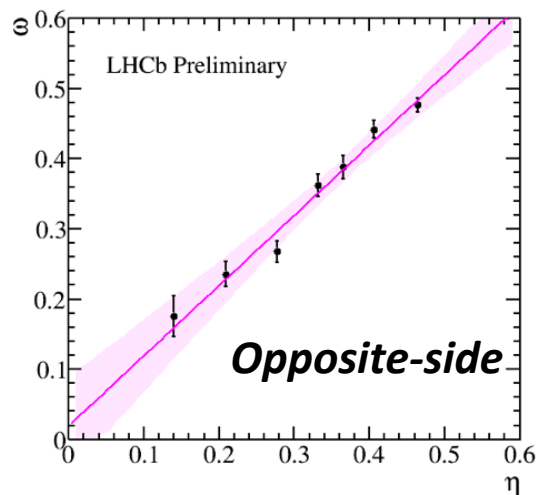


Table 1: Calibration parameters of the OS and SS taggers determined from  $B_s^0 \rightarrow D_s^- \pi^+$  decays. For  $p_0$  and  $p_1$  the first listed uncertainty is statistical and the second systematic; other parameters are not used in the fit but provided for reference only and their uncertainties, where listed, are statistical. For a perfectly calibrated tagger one expects  $p_1 = 1$  and  $p_0 - \langle \eta \rangle = 0$ .

Tagger	$p_0$	$p_1$	$\langle \eta \rangle$	$\varepsilon_{\text{tag}} [\%]$	$\varepsilon_{\text{eff}} [\%]$
OS	$0.377 \pm 0.007 \pm 0.001$	$1.12 \pm 0.08 \pm 0.01$	0.370	$37.15 \pm 0.17$	$3.55 \pm 0.33$
SS	$0.441 \pm 0.005 \pm 0.000$	$1.09 \pm 0.08 \pm 0.01$	0.437	$63.93 \pm 0.17$	$1.92 \pm 0.22$

# Correlations & Systematics

## for $B_S^0 \rightarrow D_S^\pm K^\mp$

Table 5: Total systematic uncertainties, relative to the statistical uncertainty. <sup>†</sup>The daggered contributions ( $\Gamma_s, \Delta\Gamma_s, \text{acceptance}$ ) are shown separately only for comparison. The phrase “MC ratio” refers to the ratio of  $B_S^0 \rightarrow D_S^\mp K^\pm$  and  $B_S^0 \rightarrow D_S^- \pi^+$  decay-time acceptances measured in simulated events.

Parameter	$C_f$	$A_f^{\Delta\Gamma}$	$A_{\bar{f}}^{\Delta\Gamma}$	$S_f$	$S_{\bar{f}}$
Detection asymmetry	0.01	0.23	0.26	0.02	0.03
$\Delta m_s$	0.06	0.01	0.01	0.17	0.18
Tagging and scale factor	0.15	0.06	0.06	0.22	0.16
Correlation among observables	0.27	0.25	0.18	0.20	0.23
Closure test	0.12	0.19	0.19	0.12	0.12
$\Gamma_s^\dagger$	0.02	0.16	0.18	0.01	0.01
$\Delta\Gamma_s^\dagger$	0.01	0.07	0.11	0.00	0.00
Acceptance, MC ratio <sup>†</sup>	0.04	0.09	0.10	0.01	0.01
Acceptance, data fit <sup>†</sup>	0.07	0.18	0.20	0.01	0.02
Acceptance, $\Gamma_s, \Delta\Gamma_s$	0.07	0.19	0.06	0.01	0.02
Total	0.34	0.44	0.39	0.36	0.36

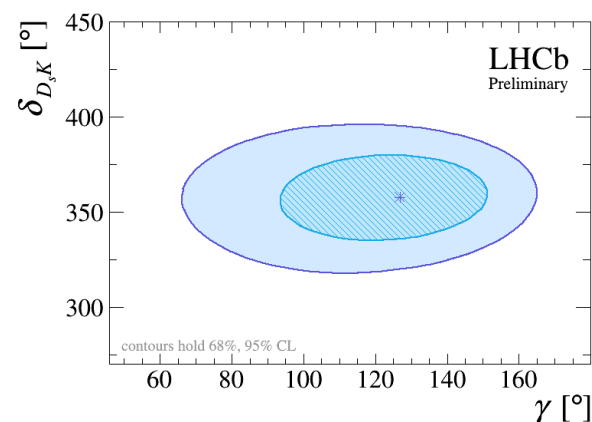
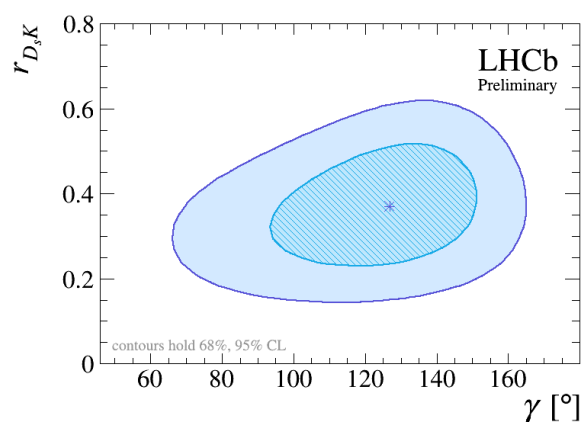
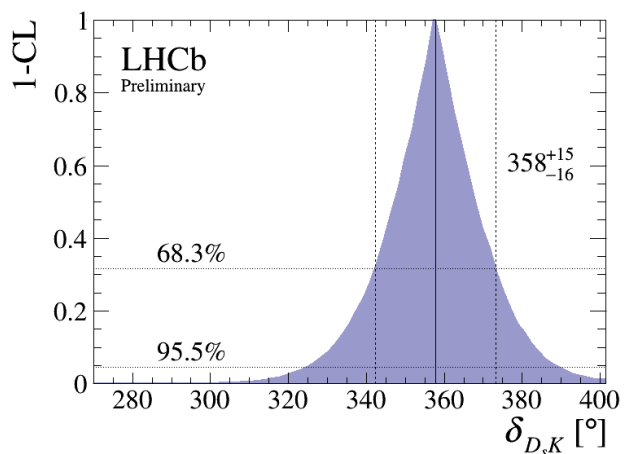
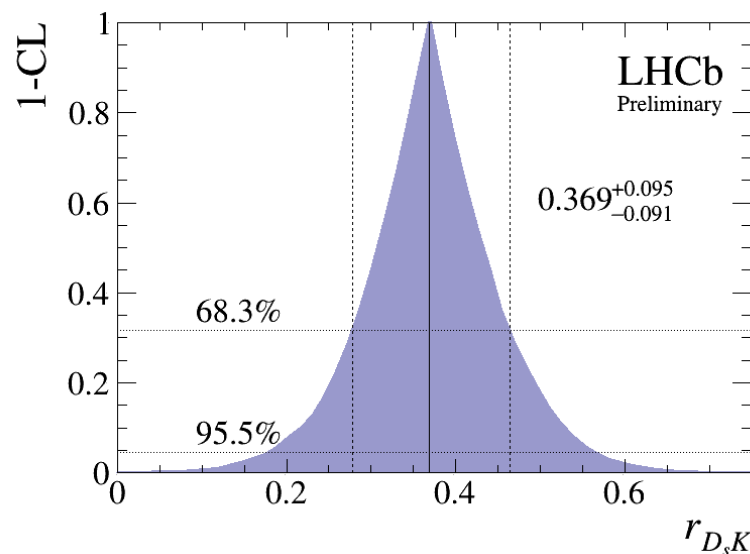
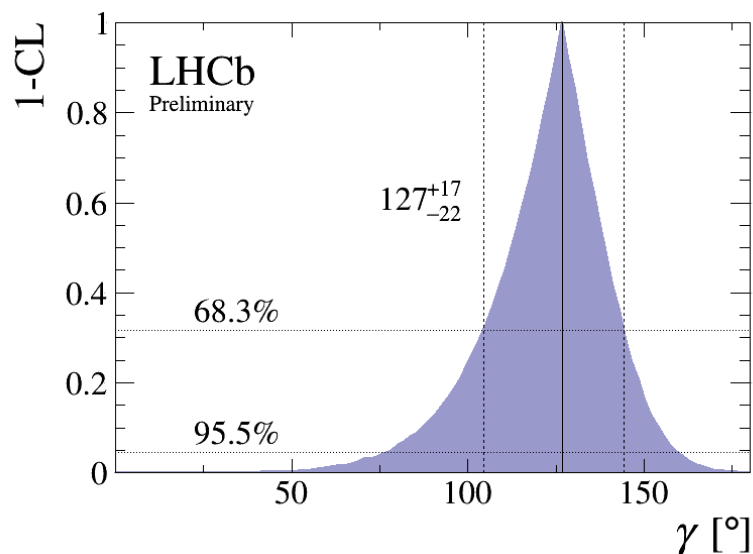
Table 4: Statistical correlation matrix of the  $CP$  parameters. Other fit parameters have negligible correlations with the  $CP$  parameters and are omitted for brevity.

Parameter	$C_f$	$A_f^{\Delta\Gamma}$	$A_{\bar{f}}^{\Delta\Gamma}$	$S_f$	$S_{\bar{f}}$
$C_f$	1.00	0.09	0.08	0.01	-0.06
$A_f^{\Delta\Gamma}$	0.09	1.00	0.51	-0.07	-0.01
$A_{\bar{f}}^{\Delta\Gamma}$	0.08	0.51	1.00	-0.03	-0.01
$S_f$	0.01	-0.07	-0.03	1.00	0.00
$S_{\bar{f}}$	-0.06	-0.01	-0.01	0.00	1.00

Table 6: Total systematic correlations.

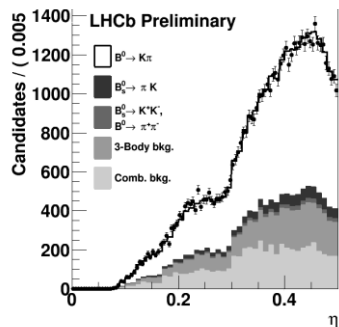
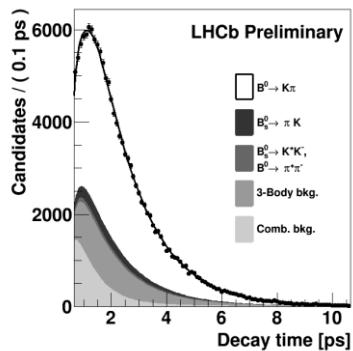
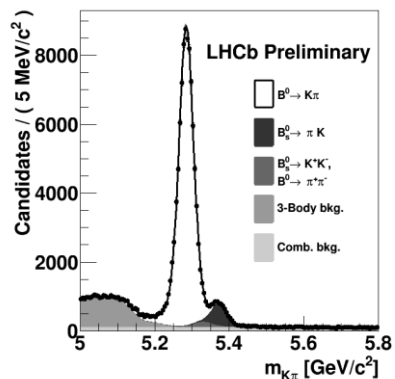
Parameter	$C_f$	$A_f^{\Delta\Gamma}$	$A_{\bar{f}}^{\Delta\Gamma}$	$S_f$	$S_{\bar{f}}$
$C_f$	1.00	0.02	0.06	0.02	0.01
$A_f^{\Delta\Gamma}$	0.02	1.00	-0.34	0.04	-0.01
$A_{\bar{f}}^{\Delta\Gamma}$	0.06	-0.34	1.00	-0.03	0.06
$S_f$	0.02	0.04	-0.03	1.00	0.00
$S_{\bar{f}}$	0.01	-0.01	0.06	0.00	1.00

# Confidence Levels for $B_S^0 \rightarrow D_S^\pm K^\mp$

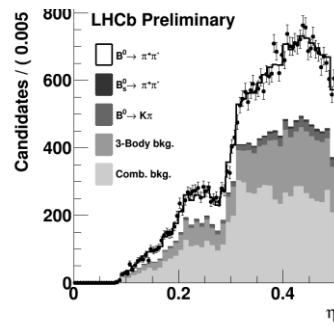
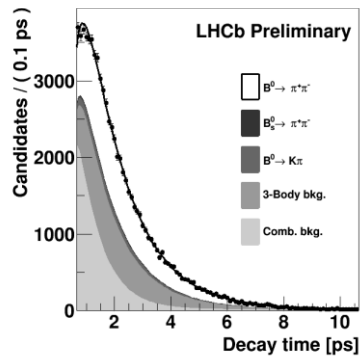
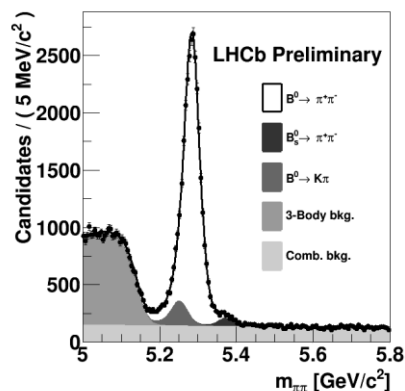


# Fits of $B_{d,s}^0 \rightarrow hh$

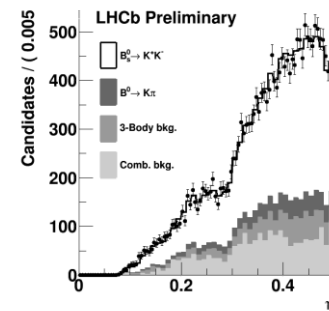
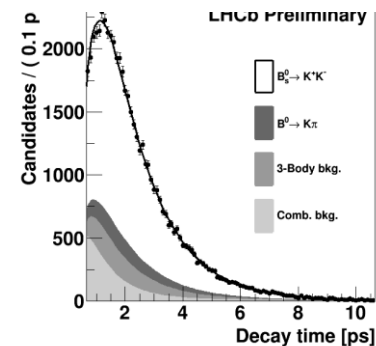
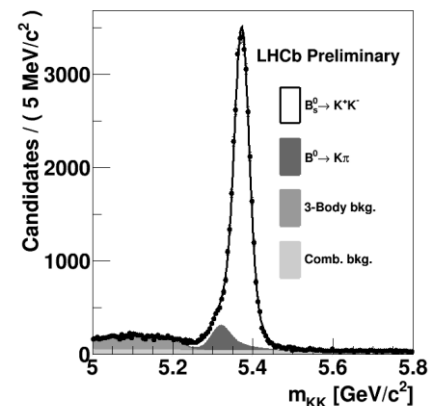
$$B_d^0 \rightarrow K^+ \pi^-$$



$$B_d^0 \rightarrow \pi^+ \pi^-$$



$$B_s^0 \rightarrow K^+ K^-$$





# Correlations & Systematics for $B_d^0 \rightarrow \pi^+ \pi^-$ and $B_s^0 \rightarrow K^+ K^-$

Table 4: Systematic uncertainties affecting the  $CP$  asymmetry coefficients of the  $B^0 \rightarrow \pi^+ \pi^-$  and  $B_s^0 \rightarrow K^+ K^-$  decays. The total systematic uncertainties are obtained by summing the individual contributions in quadrature.

Parameter	$C_{\pi^+ \pi^-}$	$S_{\pi^+ \pi^-}$	$C_{K^+ K^-}$	$S_{K^+ K^-}$	$A_{K^+ K^-}^{\Delta\Gamma}$
Time acceptance	0.001	0.001	0.003	0.003	0.093
Time resolution calibration	0.000	0.000	0.016	0.017	0.012
Time resolution model	0.000	0.000	0.007	0.008	0.000
Time error distribution	0.002	0.002	0.002	0.002	0.019
Input parameters: $\Gamma_{d,s}$ , $\Delta\Gamma_{d,s}$ , $\Delta m_{d,s}$	0.001	0.001	0.001	0.003	0.046
Tagging calibration	0.002	0.003	0.002	0.003	0.000
Cross-feed bkg. time model	0.003	0.002	0.001	0.001	0.021
Comb. and 3-body bkg. time model	0.001	0.001	0.000	0.000	0.001
Mass model	0.003	0.003	0.006	0.005	0.010
Total	0.005	0.005	0.019	0.020	0.109

Table 5: Statistical correlation matrix among the  $CP$  violation coefficients of the  $B^0 \rightarrow \pi^+ \pi^-$  and  $B_s^0 \rightarrow K^+ K^-$  decays.

Parameter	$C_{\pi^+ \pi^-}$	$S_{\pi^+ \pi^-}$	$C_{K^+ K^-}$	$S_{K^+ K^-}$	$A_{K^+ K^-}^{\Delta\Gamma}$
$C_{\pi^+ \pi^-}$	1.000	0.376	-0.009	-0.011	0.000
$S_{\pi^+ \pi^-}$	—	1.000	-0.055	-0.013	0.000
$C_{K^+ K^-}$	—	—	1.000	-0.005	0.035
$S_{K^+ K^-}$	—	—	—	1.000	0.037
$A_{K^+ K^-}^{\Delta\Gamma}$	—	—	—	—	1.000

# Constraints on $\gamma$ from $B_d^0 \rightarrow \pi^+ \pi^-$ and $B_s^0 \rightarrow K^+ K^-$

- The  $CP$  observables measured in a time-dependent analysis of  $B_d^0 \rightarrow \pi^+ \pi^-$  and  $B_s^0 \rightarrow K^+ K^-$ , using can be related to the physics parameters:

$$C_{\pi^+\pi^-} = -\frac{2d \sin(\vartheta) \sin(\gamma)}{1 - 2d \cos(\vartheta) \cos(\gamma) + d^2}, \quad S_{\pi^+\pi^-} = -\frac{\sin(2\beta + 2\gamma) - 2d \cos(\vartheta) \sin(2\beta + \gamma) + d^2 \sin(2\beta)}{1 - 2d \cos(\vartheta) \cos(\gamma) + d^2},$$

$$C_{K^+K^-} = \frac{2\tilde{d}' \sin(\vartheta') \sin(\gamma)}{1 + 2\tilde{d}' \cos(\vartheta') \cos(\gamma) + \tilde{d}'^2}, \quad S_{K^+K^-} = -\frac{\sin(-2\beta_s + 2\gamma) + 2\tilde{d}' \cos(\vartheta') \sin(-2\beta_s + \gamma) + \tilde{d}'^2 \sin(-2\beta_s)}{1 + 2\tilde{d}' \cos(\vartheta') \cos(\gamma) + \tilde{d}'^2}$$

- The parameters  $d$  and  $\theta$  are related to the “penguin to tree ratio”:

$$d^{(\prime)} e^{i\vartheta^{(\prime)}} \equiv \frac{1}{R_u} \frac{P^{(\prime)c} - P^{(\prime)t}}{T^{(\prime)} + P^{(\prime)u} - P^{(\prime)t}}, \quad \text{where} \quad R_u = \frac{1}{\lambda} \left(1 - \frac{\lambda^2}{2}\right) \left| \frac{V_{ub}}{V_{cb}} \right|$$

- To simplify the equations, we also define:  $\tilde{d}' \equiv d'(1 - \lambda^2)/\lambda^2$
- If U-spin symmetry holds, then  $d = d'$  and  $\theta = \theta'$ .
- This reduces the number of free parameters, making the system of equations soluble.

# Constraints on $\gamma$ from $B_d^0 \rightarrow \pi^+ \pi^-$ and $B_s^0 \rightarrow K^+ K^-$

- A previous LHCb paper derived constraints on  $\gamma$  using the  $CP$  observables measured in a time-dependent analysis of  $B_d^0 \rightarrow \pi^+ \pi^-$  and  $B_s^0 \rightarrow K^+ K^-$ , using 1/fb of data.

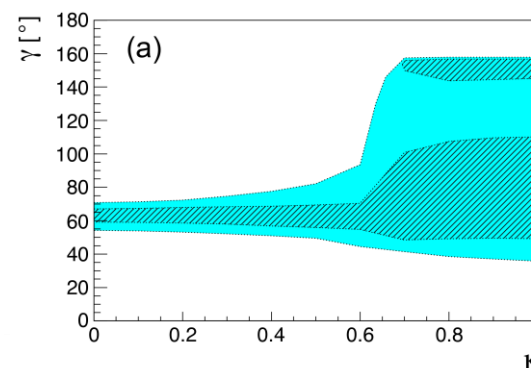
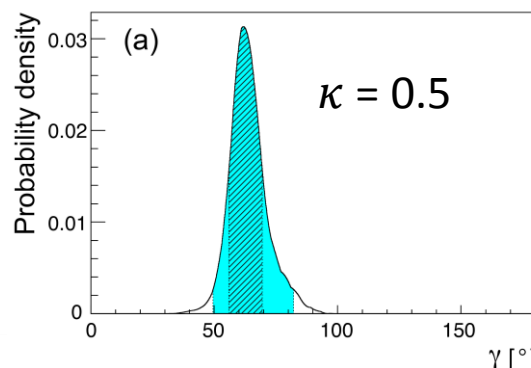
$CP$  observable results with 1/fb:

PLB **741** (2015) 1, JHEP **10** (2013) 183

$$C_{KK} = 0.14 \pm 0.11 \text{ (stat)} \pm 0.03 \text{ (syst)}, \quad C_{\pi\pi} = -0.38 \pm 0.15 \text{ (stat)} \pm 0.02 \text{ (syst)},$$

$$S_{KK} = 0.30 \pm 0.12 \text{ (stat)} \pm 0.04 \text{ (syst)}, \quad S_{\pi\pi} = -0.71 \pm 0.13 \text{ (stat)} \pm 0.02 \text{ (syst)},$$

“Standard” analysis:



$\kappa$  parameterises the allowed amount of U-spin breaking

Extended analysis, incorporating information on  $B_d^0 \rightarrow \pi^0 \pi^0$  and  $B^+ \rightarrow \pi^+ \pi^0$  decays from B-factories:

